A More General Approach to Distinguishing "Homogeneous" from "Heterogeneous" Catalysis: Discovery of Polyoxoanion- and Bu_4N^+-Stabilized, Isolable and Redissolvable, High-Reactivity $Ir_{\sim 190-450}$ Nanocluster Catalysts[1]

Yin Lin and Richard G. Finke*

Department of Chemistry, Colorado State University, Ft. Collins, Colorado 80523

Received May 10, 1994[⊗]

A more general approach to distinguishing between so-called homogeneous vs heterogeneous catalysts has been developed and intrinsically tested in answering the question "what is the true catalyst in the active hydrogenation system which evolves from cyclohexene, hydrogen, and the discrete, polyoxoanion-supported Ir(I) catalyst precursor $(Bu_4N)_5Na_3[(1,5\text{-COD})IrP_2W_{15}Nb_3O_{62}]$?". The approach developed and utilized consists of four categories of experiments: (i) catalyst isolation and characterization studies, with an emphasis initially on TEM (transmission electron microscopy); (ii) initial kinetic studies, emphasizing whether or not the isolated catalyst can account for the observed kinetics, especially any induction period seen, and whether or not the reaction exhibits a ±10% reproducible rate; (iii) quantitative phenomenological catalyst poisoning and recovery experiments; (iv) additional kinetic and mechanistic studies and chemical tests, all interpreted with strict adherence to the principle that the correct description of the catalyst (i.e., the correct mechanism) will explain *all* of the data. The present approach has identified a previously unknown type of hybrid homogeneous−heterogeneous, $Ir_{\sim 190-450}$•polyoxoanion/Bu_4N^+ catalyst of *average* composition $[Ir(0)_{\sim 300}(P_4W_{30}Nb_6O_{123}{}^{16-})_{\sim 33}](Bu_4N)_{\sim 300}Na_{\sim 233}$. The discovery of, and ability to distinguish, even an unprecedented hybrid homogeneous−heterogeneous catalyst strongly suggests that the present approach will be more generally applicable to the difficult and often unsolved mechanistic problem of distinguishing catalysis by a discrete, homogeneous metal complex vs that by a soluble metal nanocluster or colloid "heterogeneous" catalyst. Some false starts and incorrect leads in the early stages of this work are discussed, research which illustrates some of the pitfalls to be avoided in attempts to distinguish homogeneous from heterogeneous catalysts. A minimum mechanistic scheme for the catalyst's evolution, consisting of the autocatalytic generation of the $Ir_{\sim 190-450}$ nanoclusters, is shown to account for all of the observed results, including the findings of the rate-enhancing effects of H^+, H_2O, and acetone impurities that were puzzling in the earlier stages of this work, before the $Ir_{\sim 190-450}$ nanocluster catalysts were identified.

Introduction

Polyoxoanions[2] are soluble metal oxide analogs[2c] that are of considerable interest as discrete oxide-support materials for transition metal organometallics[3,4] or, as discovered via the methodology developed herein, as catalyst precursors to new and reactive catalyst compositions.[5] Our approach to developing new catalysts using polyoxoanions is entering its second decade, research that has required simultaneous efforts in the four areas of reactive [e.g., M(1,5-COD), M = Ir, Rh] precatalyst synthesis,[4,6] unequivocal characterization studies,[6a−c] catalytic investigations[5,7−9] (including two patents[5b,7b]), and kinetic and mechanistic studies.[8,9] The efforts of several Ph.D. theses,[7,8,9]

⊗ Abstract published in *Advance ACS Abstracts,* September 1, 1994.

(1) Lin, Y.; Finke, R. G. Novel Polyoxoanion and Bu_4N^+ Stabilized, Isolable and Redissolvable, 20−30 Å $Ir_{\sim 300-900}$ Nanoclusters: The Kinetically Controlled Synthesis and Mechanism of Formation of Organic Solvent-Soluble, Reproducible Size and Reproducible Catalytic Activity Metal Nanoclusters. *J. Am. Chem. Soc.*, in press.

(2) (a) Pope, M. T. *Heteropoly and Isopoly Oxometalates*; Springer-Verlag: Berlin, 1983. (b) Day, V. W.; Klemperer, W. G. *Science* **1985**, *228*, 533−41. (c) Pope, M. T.; Müller, A. *Angew. Chem., Int. Ed. Engl.* **1991**, *30*, 34. (d) Baker, L. C. W. In *Advances in the Chemistry of Coordination Compounds*; Kirschner, S., Ed.; MacMillan: New York, 1961; p 604.

(3) Organometallic derivatives of polyoxoanions, unknown a decade ago, are now relatively common. However, still in their infancy are reactivity, catalysis, and mechanistic studies of polyoxoanion-based materials. (a) Reference 2a and the references therein. (b) Klemperer, W. G.; Yagasaki, A. *Chem. Lett.* **1989**, 2041. (c) Day, V. W.; Klemperer, W. G.; Yagasaki, A. *Chem. Lett.* **1990**, 1267. (d) Day, V. W.; Klemperer, W. G.; Main, D. J. *Inorg. Chem.* **1990**, *29*, 2345−55. (e) Klemperer, W. G.; Main, D. J. *Inorg. Chem.* **1990**, *29*, 2355−60.

(4) (a) Finke, R. G.; Droege, M. W. *J. Am. Chem. Soc.* **1984**, *106*, 7274−7. (b) Edlund, D. J.; Saxton, R. J.; Lyon, D. K.; Finke, R. G. *Organometallics* **1988**, *7*, 1692−704. (c) Finke, R. G.; Rapko, B.; Domaille, P. J. *Organometallics* **1986**, *5*, 175−8.

(5) For catalysis under oxidative conditions,[5a,b] where analogous mechanistic studies indicate the catalyst remains polyoxoanion-supported,[5c] see: (a) Mizuno, N.; Lyon, D. K.; Finke, R. G. *J. Catal.* **1991**, *128*, 84−91. (b) Mizuno, N.; Lyon, D. K.; Finke, R. G., U.S. Patent 5,250,739, Oct. 5, 1993. (c) Trovarelli, A.; Weiner, H.; Lin, Y.; Finke, R. G. Manuscript in preparation.

(6) (a) Finke, R. G.; Lyon, D. K.; Nomiya, K.; Sur, S.; Mizuno, N. *Inorg. Chem.* **1990**, *29*, 1784−7. (b) Pohl, M.; Finke, R. G. *Organometallics* **1993**, *12*, 1453. (c) Pohl, M.; Lyon, D. K.; Mizuno, N.; Nomiya, K.; Finke, R. G. Polyoxoanion-Supported Catalyst Precursors. Synthesis and Characterization of the Iridium(I) and Rhodium(I) Precatalysts $[(n\text{-}C_4H_9)_4N]_5Na_3[(1,5\text{-COD})M•P_2W_{15}Nb_3O_{62}]$ (M = Ir, Rh). *Inorg. Chem.*, submitted for publication. (d) Nomiya, K.; Mizuno, N.; Lyon, D. K.; Finke, R. G. Polyoxoanion-Supported, Atomically Dispersed Iridium(I) and Rhodium(I). *Inorg. Synth.*, in press.

(7) (a) Edlund, D. J. Ph.D. Dissertation, University of Oregon, September 1987. (b) A patent based primarily on this thesis has been issued: Edlund, D. J.; Finke, R. G.; Saxton, R. J. U.S. Patent 5,116,796, May 26, 1992.

(8) (a) Lyon, D. K. Ph.D. Dissertation, University of Oregon, September 1990. (b) There are several errors in the experiments, and thus also in the interpretations, reported in this thesis.[8a] *Note that it is crucial to be able to explain all the earlier observations, errors, and misinterpretations as well,[8a] since only then can we be sure that the full and complete mechanistic picture is in hand.* For this reason, the errors and misinterpretations elsewhere[8a] are enumerated, corrected, and discussed in the supplementary material of another, subsequent thesis.[9] (c) Despite these errors,[8b] the thesis in question[8a] still contains a number of interesting reports that, *if and when they prove repeatable*, may provide interesting insights into chemistry and mechanisms of the novel polyoxoanion-stabilized $Ir_{\sim 190-450}$ clusters discovered via this work. Repeating and verifying those results is one of our current goals.

0020-1669/94/1333-4891$04.50/0

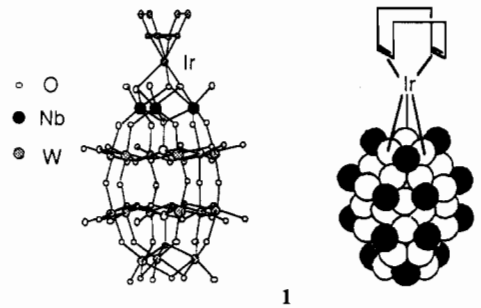

1

Figure 1. Ball and stick (leftmost) and space-filling (rightmost) representations of $(Bu_4N)_5Na_3[(1,5\text{-COD})Ir{\cdot}P_2W_{15}Nb_3O_{62}]$, **1**, as characterized elsewhere.[6] In the space-filling representation the black circles represent terminal M=O oxygens, while the open, white circles represent M−O−M bridging oxygens.

often checking and re-investigating[9] initial observations[7,8] or interpretations,[7,8,10] have been required to bring the catalytic and mechanistic studies summarized herein to completion. It merits noting that the custom-made, highly basic $P_2W_{15}Nb_3O_{62}^{9-}$ polyoxoanion employed herein is arguably the premier polyoxoanion-support system presently available for such studies[3,4,6] in that it exhibits 1:1 organometallic:polyoxoanion complexes that are often single, regiospecific support-site isomers, as is the case for the supported iridium(I) complex[6] $(Bu_4N)_5Na_3[(1,5\text{-COD})Ir{\cdot}P_2W_{15}Nb_3O_{62}]$, **1**, employed herein, Figure 1.

Two early, key conceptual decision points in designing these studies proved, as expected, to be (i) the choice of a simple, well-studied catalytic reaction for our initial catalytic survey reactions[11] [catalytic hydrogenations, one of the oldest and best studied catalytic reactions[12] (but a technologically significant reaction, one where commercial opportunities for new catalysts still exist[12m])] and (ii) an emphasis, both initially and then throughout these studies, upon chemical kinetics, since catalysis is by definition a wholly kinetic phenomenon.[13]

Throughout this work we will employ Schwartz's more modern definitions[14] of "homogeneous" and "heterogeneous" catalysts. Schwartz's definitions replace the classical, solubility-based definitions that equate "heterogeneous" with "insoluble" and "homogeneous" with "soluble" but which say nothing about the *more important issue* of the homogeneity or heterogeneity of the catalysts' active site(s). Schwartz's definition deals with the active site issue by equating, instead, a homogeneous catalyst as one that has uniformity (homogeneity) in its active sites, while a heterogeneous catalyst is one that has a multitude of (different; heterogeneous) active sites (Figure 2).

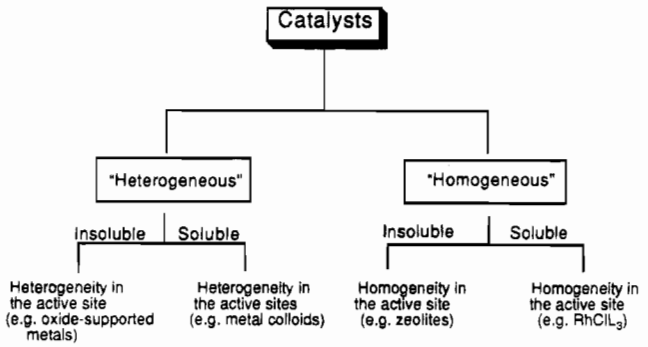

Figure 2. Revised classification of "homogeneous" vs "heterogeneous" catalysts (adapted and expanded following Schwartz's suggestions[14]). This classification scheme emphasizes the (harder to determine) homogeneous vs heterogeneous nature of the active site over the (more easily determined) solubility or insolubility of the catalyst, since the former is more crucial in determining the catalyst's selectivity.

Another required definition for the present studies, one that is mildly controversial,[15a] is the distinction between a classical metal "colloid" and metal "nanoclusters". We will follow Schmid here,[15b] who defines metal clusters (including nanoscale, "nanoclusters") as those metal aggregates smaller than 100 Å (i.e., 10 Å) and colloids as those aggregates larger than 100 Å (which also tend to have a broader size distribution). Note that there is really no need for controversy here once one realizes that *a continuum* of cluster sizes is expected (see footnote 9 elsewhere[1]).

Previous Approaches to the Problem of Distinguishing Homogeneous vs Heterogeneous Catalysts

A concise summary of the prior literature focused on the "homogeneous vs heterogeneous" problem[16-27] (see Table A,

(9) Lin, Y. Ph.D. Dissertation, Department of Chemistry, University of Oregon, March 1994.

(10) (a) A preliminary account of our initial mechanistic studies: Lyon, D. K.; Finke, R. G. *Inorg. Chem.* **1990**, *29*, 1787−9. (b) While at that time, and on the basis of the available evidence[8] (especially a flawed solution MW experiment that is corrected herein), we favored a discrete polyoxoanion-supported homogeneous catalyst, we did correctly note, as our bottom-line and italicized conclusion, the still true finding that the data only required, rigorously, that some type of "*Ir to polyoxoanion bonding be retained in the catalyst derived from I*" (see p 1789). We also noted, as has indeed proved true, that one of the possibilities was that "we have discovered a previously unknown polyoxoanion-supported and stabilized "colloid" of a highly uniform and thus novel type" (see p 1788, footnote 13).

(11) Indeed, hindsight has confirmed our early intuition and conservative approach: it would have been a mistake to choose a more challenging reaction (i.e., before demonstrating the true identity of the catalyst derived from $(Bu_4N)_5Na_3[(1,5\text{-COD})Ir{\cdot}P_2W_{15}Nb_3O_{62}]$ for different reactions and conditions). Fortification for this statement comes from the fact that the extensive mechanistic work reported herein has been required to establish the true nature of the (previously unknown) Bu_4N^+/polyoxoanion-stabilized $Ir_{\sim 300}$ nanocluster catalyst even for the relatively straightforward case of catalytic hydrogenations. Hence, logic dictates that an even more difficult time would have been the case if a more complicated, and less well characterized, reaction had been chosen initially.

(12) Reviews concerning homogeneous hydrogenation include: (a) James, B. R. In *Homogeneous Hydrogenation*; Wiley: New York, 1974. (b) James, B. R. *Adv. Organomet. Chem.* **1979**, *17*, 319. (c) Birch, A. D.; Williamson, D. H. *Org. React.* **1976**, *24*, 1. (d) Jardine, F. H. *Prog. Inorg. Chem.* **1981**, *28*, 63. (e) Faller, J. W. In *Homogeneous Catalysis with Metal Phosphine Complexes*; Pignolet, L. H., Ed.; Plenum: New York, 1983; Chapter 2. (f) James, B. R. In *Comprehensive Organometallic Chemistry*; Wilkinson, G., Stone, F. G. A., Abel, E. W., Eds.; Pergamon: New York, 1982; Vol. 8, p 285. (g) Reference 23, p 523. (h) Reviews concerning asymmetric homogeneous hydrogenations include: (i) Kagan, H. B.; Frian, J. C. *Top. Stereochem.* **1977**, *10*, 175. (j) Morrison, J. D.; Masler, W. F.; Neuberg, M. K. *Adv. Catal.* **1976**, *25*, 81. (k) Valentine, D.; Scott, J. W. *Synthesis* **1978**, 329. (l) Morrison, J. D.; Masler, W. F.; Hathaway, S. In *Catalysis in Organic Synthesis*; Rylander, P. N., Greenfield, H., Eds.; Academic: New York, 1976. (m) Opportunities for new, selective hydrogenation catalysts still exist: Catalytica, Inc., personal communication (Multiclient study no. 4188CH, Selective Catalytic Hydrogenation). See also: *Chem. Eng. News* **1989**, *42*, (May 29), 40.

(13) (a) Halpern, J.; Okamoto, T.; Zakhariev, A. *J. Mol. Cat.* **1976**, *2*, *65*. (b) Halpern, J. *Inorg. Chim. Acta* **1981**, *50*, 11.

(14) Schwartz, J. *Acc. Chem. Res.* **1985**, *18*, 302.

(15) (a) See footnote 9 and Bradley's discussion (ref 7) provided elsewhere.[1] (b) Schmid, G. *Endeavour* **1990**, *14*, 172.

(16) Hamlin, J. E.; Hirai, K.; Millan, A.; Maitlis, P. M. *J. Mol. Catal.* **1980**, *7*, 543.

(17) Foley, P.; DiCosimo, R.; Whitesides, G. M. *J. Am. Chem. Soc.* **1980**, *102*, 6713.

(18) Laine, R. *J. Mol. Catal.* **1982**, *14*, 137.

(19) (a) Crabtree, R. H.; Mihelcic, J. M.; Quirk, J. M. *J. Am. Chem. Soc.* **1979**, *101*, 7738. Crabtree, R. H.; Mellea, M. F.; Mihelcic, J. M.; Quirk, J. M. *J. Am. Chem. Soc.* **1982**, *104*, 107. (b) Anton, D. R.; Crabtree, R. H. *Organometallics* **1983**, *2*, 855.

(20) Collman, J. P.; Kosydar, K. M.; Bressan, M.; Lamanna, W.; Garrett, T. *J. Am. Chem. Soc.* **1984**, *106*, 2569.

(21) Whitesides, G. M.; Hackett, M.; Brainard, R. L.; Lavalleye, J.-P. P. M.; Sowinski, A. F.; Izumi, A. N.; Moore, S. S.; Brown, D. W.; Staudt, E. M. *Organometallics* **1985**, *4*, 1819.

(22) Crabtree, R. H. *Chem. Rev.* **1985**, *85*, p 245.

(23) Collman, J. P.; Hegedus, L. S.; Norton, J. R.; Finke, R. G. *Principles and Applications of Organotransition Metal Chemistry;* University Science Books: Mill Valley, CA, 1987; p 561.

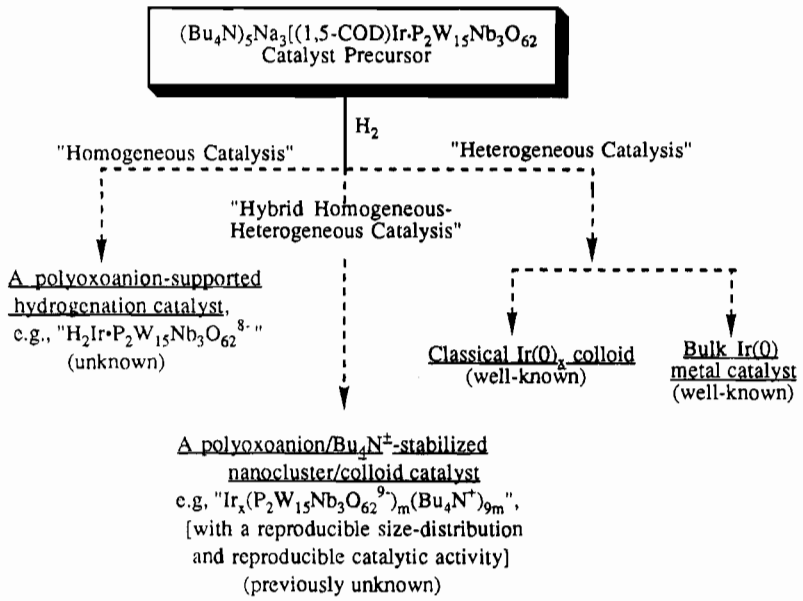

Figure 3. Three limiting mechanistic hypotheses for the hydrogenation catalyst derived from $(1,5\text{-COD})Ir{\cdot}P_2W_{15}Nb_3O_{62}^{8-}$, **1**.

supplementary material) reveals a number of insights. Specifically, the highlights from a perusal of the relevant literature, plus insights generated via the studies presented herein, are ninefold: (i) So far, no single technique has been able to provide an unambiguous answer to the "homogeneous vs heterogeneous" question for all systems examined. (ii) Instead, a range of physical methods and tests must be used as Crabtree has emphasized[19b] (and the phenomenological tests are likely to be ambiguous unless used *quantitatively* and with the proper controls, e.g., the controls needed herein as part of the Hg test experiments). (iii) TEM is, as Lewis' recent results[24,25] plus the results herein show, the single most valuable and easiest to use technique, one that has been grossly underutilized previously in examining the homogeneous vs heterogeneous catalysis question (and one that should be used in a re-examination of two catalysts[26,27] claimed to be "homogeneous"). Further highlights from the relevant literature are as follows. (iv) Kinetic studies are a required but again underutilized tool, one that must be an integral part of any attempt to identify the active catalyst (of any catalytic reaction[13]). (v) An observation of an induction period *in reductive catalysis* is quite suggestive of (but not proof of) the formation of metal colloid or nanocluster particles. (vi) The Hg poisoning test appears to be a quite valuable test, as long as any necessary control experiments are also performed. (vii) In one case, an opposite conclusion has been reached by different workers examining the same catalyst but using different methods (entries 5 and 6, Table A). Final insights from the literature include the following. (viii) The classic prior studies are probably the 1980 Whitesides Hg test papers,[17,21] the 1979–1982 Crabtree study[19] (providing evidence for a *homogeneous* hydrogenation catalyst), and then the 1986 Lewis and Lewis study and subsequent papers[24,25] (providing strong evidence for a *heterogeneous*, colloidal Pt_x hydrosilylation catalyst). (ix) However, in arguably none of the prior studies has *a more general solution* to the often difficult if not perplexing "homogeneous vs heterogeneous" mechanism problem appeared. Certainly, there is no prior study of this central mechanistic problem in homogeneous and heterogeneous catalysis that has been developed—and intrinsically tested—through the discovery of a previously unknown type of "hybrid homogeneous–heterogeneous" catalyst (i.e., one with key features from *both* types of catalysts) such as the polyoxoanion and Bu_4N^+ stabilized $Ir_{\sim 190-450}$ nanolcuster catalysts discovered herein.

Approach Used in the Present Studies

Our own work began with the goal of answering the question "what is the true catalyst in the hydrogenation reactions beginning with $(Bu_4N)_5Na_3[(1,5\text{-COD})Ir{\cdot}P_2W_{15}Nb_3O_{62}]$, **1**?" At the very beginning of these studies back before 1985 (and, at that time with the Rh analog of **1**),[7a] the primary focus of these studies was to provide evidence for or against a "homogeneous vs a heterogeneous" species as the true catalyst, Figure 3. We were especially cognizant that what one then termed a "metal colloid" was a very likely candidate for the true catalyst. As these studies progressed, we realized that a third possibility was a hybrid "homogeneous/heterogeneous" catalyst, one that has key features of *both* traditional heterogeneous colloids and discrete, homogeneous catalysts, Figure 3.

During our studies, it became clear that the level of effort and detail that were required might also allow us to develop a more general approach to the "homogeneous vs heterogeneous" problem. The successful approach that we developed is summarized in Figure 4, in a somewhat hindsight-optimized order of classes of experiments, 1–4. Noteworthy in Figure 4 is the emphasis initially upon catalyst isolation and TEM studies (plus other, multiple physical tools), then kinetic studies probing the reaction's reproducibility, followed by *quantitative* catalyst poisoning and recovery studies, and finally additional quantitative kinetic and mechanistic studies *until a completely consistent picture and mechanism that explains all the observed data is obtained* (e.g., the effects of H_2O documented herein). In hindsight, three reasons that the extensive studies reported herein were required are as follows:[28a] (i) Good examples of zerovalent transition metal nanocluster catalysts, which could be isolated with virtually no aggregation and then redissolved at will in organic solvents, were unknown until well into the present studies.[29] (ii) The *polyoxoanion-dispersed and stabilized* $Ir(0)_{\sim 190-450}$ nanocluster catalysts discovered via the methods developed herein were without prior precedent.[1] (iii) It was

(24) Lewis, L. N.; Lewis, N. *J. Am. Chem. Soc.* **1986**, *108*, 7228.
(25) (a) Lewis, L. N. *J. Am. Chem. Soc.* **1986**, *108*, 743. (b) Lewis, L. N.; Lewis, N.; Uriarte, R. J. In *Advances in Chemistry Series*; Moser, W. R., Slocum, D. W., Eds.; American Chemical Society: Washington, DC, 1992; Vol. 230, p 541. (c) Lewis, L. N. *J. Am. Chem. Soc.* **1990**, *112*, 5998. (d) Lewis, L. N.; Lewis, N. *Chem. Mater.* **1989**, *1*, 106.
(26) van Asselt, R.; Elsevier, C. J. *J. Mol. Catal.* **1991**, *65*, L13–L19.
(27) Coqueret, X.; Wegner, G. *Organometallics* **1991**, *10*, 3139.

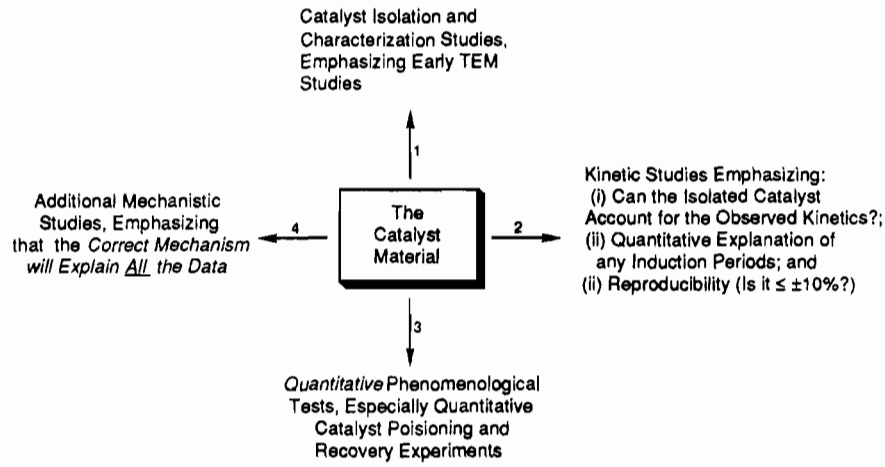

Figure 4. A successful approach to distinguishing between a "heterogeneous" colloid-nanocluster catalyst and a discrete, "homogeneous" polyoxoanion-supported catalyst.

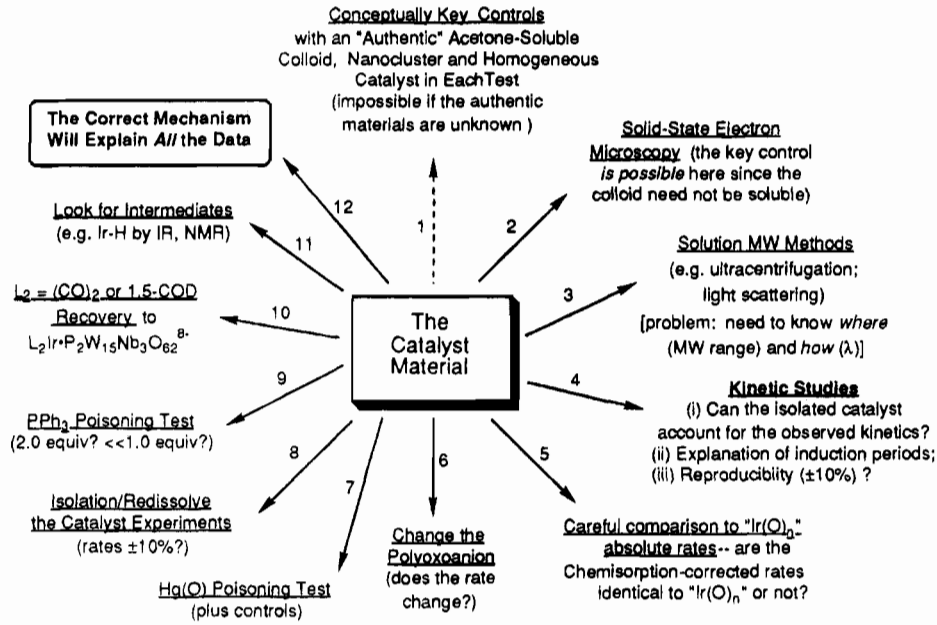

Figure 5. An optimized, more general approach to distinguishing homogeneous from heterogeneous catalysts.

mistakenly believed in the literature, and thus initially by us as well, that "heterogeneous" nanocluster or colloid catalysts could not have a kinetic reproducibility ≤10%, a myth[28b] disproven by the present work.

If we expand upon Figure 4, the specific questions asked and experiments performed, again in a somewhat hindsight-optimized organization, are summarized in Figure 5, a figure which also serves as a concise introduction to the Results and Discussion section and its organization. Two points regarding Figure 5 merit mention before proceeding to the key results. First, a simple but key conceptual point (item no. 1, Figure 5) is that one should, where possible, examine *up front* each possible type of known and available (and isolable) homogeneous or heterogeneous catalyst (i.e., in key control experiments comparing the catalyst in question to each known catalyst type, using each physical method or test). Unfortunately, this idealized approach is probably rarely possible since the true catalyst may not be isolable and may even be unprecedented. (In the present study, two of the four catalysts suggested in Figure 5 were unknown when we began, making the "homogeneous vs heterogeneous" question much more challenging to address definitively.)

This brings up the second prefacing point regarding Figure 5: note that electron microscopy (i.e., TEM) completely avoids any problems with the solubility of a given colloid. That is, since *water-soluble* Ir_x nanocluster/colloids are known, they could be (and were) used in an early control experiment to obtain a TEM in the *solid-state* of an authentic, acetone (i.e., non-aqueous) soluble Ir_x nanocluster/colloid. Figures 4 and 5 summarize the highlights of the present, nearly decade long mechanistic study. The interested reader is directed to a brief review, available elsewhere as part of a symposium proceedings,[30] for a summary of our reductive and oxidative[30b] catalysis and mechanistic work using the precatalyst $(Bu_4N)_5Na_3[(1,5\text{-}COD)Ir{\cdot}P_2W_{15}Nb_3O_{62}]$, **1**.

Results and Discussion

(1) Cyclohexene Hydrogenation as a Prototype Catalytic Reaction. (A) Hydrogenation Apparatus and "Standard

(28) (a) A fourth reason is the failure of our early work[8a,10a] to emphasize catalyst isolation and characterization studies, especially by TEM, something that is, however, now properly emphasized in Figure 4 and is inherently built into Figure 5. (b) For example note the quote provided elsewhere:[28c] "Note also that a true homogeneous catalyst usually demonstrates a notably better reproducibility in the values of reaction rate than a catalyst whose activity arises from its decomposition into a colloidal metal. *This difference in reproducibility can also be used to distinguish between the two types of catalysis*". (c) The Chemistry and Physics of Small Metallic Particles. *Faraday Discuss.* **1991**, *92*, 79−107 and see p 102.

Conditions" for Cyclohexene Hydrogenation. A prototype catalytic reaction, the hydrogenation of cyclohexene, was chosen for study. It was typically carried out using a set of conditions and procedures referred to hereafter as the "Standard Conditions" for cyclohexene hydrogenation, namely 1.2 mM of well-characterized $(Bu_4N)_5Na_3[(1,5\text{-COD})Ir{\cdot}P_2W_{15}Nb_3O_{62}]$, **1**,[6] as the precatalyst, 1.65 M purified cyclohexene, 40 psig H_2, 22.0 ± 0.1 °C, and relatively "dry" Burdick & Jackson acetone as solvent (containing 0.2% water, i.e., 0.10 M or 85 equiv of H_2O vs **1**). The hydrogenation reaction was monitored by its H_2 pressure loss as detected by a precise (±0.1 psig) pressure transducer interfaced to an IBM-compatible computer, as the schematic in Figure 6 illustrates. The Swagelock "quick-connects" are a nice feature of the hydrogenation apparatus shown in Figure 6, as they allow the Fischer-Porter bottle to be filled with the reactants and catalyst under strict, ≤1 ppm O_2-free conditions in an inert-atmosphere drybox. As noted elsewhere,[1] a failure to exclude O_2 is a design flaw in probably three-fourths of the earlier literature of metal nanoclusters or colloids.

Several types of control experiments were also done which demonstrate that the hydrogenation apparatus performed as desired. Specifically, control experiments were done demonstrating that (i) the apparatus did not admit detectable (≪1 mM) amounts of air/O_2 over the time course of the hydrogenation experiments (<15 h), (ii) the apparatus correctly reproduces an independently measured hydrogenation rate for a known catalyst, Crabtree's $[Ir(1,5\text{-COD})(PPh_3)_2]^+PF_6^-$, and (iii) the Fischer-Porter bottle and pressure apparatus did not leak appreciable H_2 during a typical (Standard Conditions) hydrogenation experiment (i.e., over ca. 10 h). Precautions were also taken to ensure that trace metal precipitates or contaminates did not contribute to the results reported herein. Specifically, the borosilicate liner and reaction (culture) tubes used, Figure 6, were disposed of after each run, and the stir bars added to the culture tubes were shown to be free of catalytically active precipitates in control experiments.

Overall, then, five types of control experiments were done to ensure that the hydrogenation apparatus shown in Figure 6 provides a high-precision, accurate record of the desired hydrogenation reaction under conditions where oxygen is excluded to a level ≪1 mM.

(B) Stoichiometry. Hydrogenation Reaction and Evolution of Cyclooctane from Reduction of 1,5-COD in the Precatalyst, $(Bu_4N)_5Na_3[(1,5\text{-COD})Ir{\cdot}P_2W_{15}Nb_3O_{62}]$, 1. As shown in Figure 7, a Standard Conditions cyclohexene hydrogenation, employing $(Bu_4N)_5Na_3[(1,5\text{-COD})Ir{\cdot}P_2W_{15}Nb_3O_{62}]$, **1**, as the precatalyst, proceeds with a reproducible 2.0 ± 0.2 h induction period (the induction period is defined operationally as the time after which a 0.05 psig H_2 loss/2.5 min is observed). The reaction then "turns on", in what has been previously shown to be quantitatively fit *only* by autocatalysis,[1,10] that is, by the step 1 catalyst + **1** + $3.5H_2$ → 2 catalyst. Following the autocatalytic "burst" of activity, a roughly linear section in the H_2 uptake curve is seen, Figure 7. (However, caution must be exercised in interpreting this linear, apparently "zero-order in H_2" section of the $\{-d[H_2]/dt\}_{apparent}$ since catalyst is still being produced, *vide infra*, and thus the reaction would go even faster and faster were it not for the decrease in $P(H_2)$ and [cyclohexene] and, thus, their implied non-zero-order rate dependence.) The Standard Conditions hydrogenation reaction shown in Figure 7 is effectively finished in another 5−6 h (8 h total), during which ca. 1400 catalyst cycles have occurred. GLC and NMR confirm that 100% of cyclohexane has been produced, eq 1b. Overall, and as eq 1 indicates, 3.5 equiv of H_2 is required[1]

$$(1,5\text{-COD})Ir{\cdot}P_2W_{15}Nb_3O_{62}^{8-} + 3.5\ H_2 \xrightarrow{\text{acetone, 22 °C}} \bigcirc + \text{CATALYST} \quad (1a)$$

(Precatalyst, 1) (1.0 equiv)

$$\bigcirc + H_2 \xrightarrow[\text{CATALYST}]{\text{acetone, 22 °C}} \bigcirc \quad (1b)$$

to yield the active catalyst from **1**. Careful visual observation of the reaction solution shows that, as the reaction proceeds, the originally clear-yellow reaction solution gradually turns turbid yellow-brown, but bulk, insoluble Ir(0) metal particles are never observed. Also, when ca. 90% of the cyclohexene has been converted to cyclohexane, the reaction solution turns an intense blue color, which has been shown to be due to the reduction of the polyoxoanion to a W^V-containing "heteropolyblue".[1] Since the heteropolyblue formation is known to be of no consequence to the hydrogenation reaction (other than it consumes 1.0 equiv of H_2 of the reaction shown in eq 1a),[1] the heteropolyblue formation need not be of further concern for the purposes of the present paper.

One important issue, which was not at all clear initially, was that of how long it takes for all the precatalyst **1** to evolve into the active catalyst. By the use of carefully designed experiments (five independent reactions, one for each point in Figure 7, inset), and the use of both internal standard and absolute calibration-curve quantitation in the GLC experiments, it was shown that it takes a full ca. 8−10 h for the production of 1.0 equiv of cyclooctane and thus for the precatalyst **1** to evolve fully into the active catalyst. This required 8−10 h is 4−5 times slower than the ca. 2 h induction period, *so that even after 6 h, only ca. 45% of the 1,5-cyclooctadiene in 1 has been released as cyclooctane; during this time, however, ca. 85% of the cyclohexene has already been hydrogenated.* This result confirms what the observation of autocatalysis also indicates, that a highly active catalyst is produced from a small fraction of **1** being converted into the true catalyst (and that the true

(29) While a more comprehensive list of recent literature in the nanocluster/colloid literature is available in an accompanying paper[1] and an earlier communication,[10a] recent noteworthy papers reporting highly stablilized and isolable/redissolvable nanoclusters are summarized below. (a) An Ir colloid that is soluble in acetone and is $(octyl)_4N^+$ stabilized: Bönnemann, H.; Brijoux, W.; Brinkmann, R.; Dinjus, E.; Joussen, K. B. *Angew. Chem., Int. Ed. Engl.* **1991**, *30*, 1312. (b) Very recently Klabunde and co-workers have described soluble 10−20 Å nonuniform metal/perfluorocarbon clusters of *average* formula $Au_{17}[C_{20}H_{30}F_{26}NO_7]$ prepared from condensing Au atoms with $(CF_3CF_2CF_2)_3N$. The surface of these clusters reacts with, and apparently is protected by, the "$C_{20}H_{30}F_{26}NO_7$" fragment of unknown structure(s). Hence the finding that they can be taken to dryness and then redissolved in solvents that include acetone is probably not relevant to the present work (where Ir is exposed and reactive): Zuckerman, E. B.; Klabunde, K. J.; Olivier, B. J.; Sorensen, C. M. *Chem. Mater.* **1989**, *1*, 12−14. (c) Vargaftik, M. N.; Zagorodnikov, V. P.; Stolyarov, I. P.; Moiseev, I. I.; Kochubey, D. I.; Likholobov, U. A.; Chuvilin, A. L.; Zamaraev, K. I. *J. Mol. Cat.* **1989**, *53*, 315. The distribution of clusters therein, approximated by "$Pd_{\sim 561}phen_{60}O_{60}(PF_6)_{60}$", shows a molecular weight of (1.0 ± 0.5) × 10^5 g/mol by ultracentrifugation sedimentation velocity. (d) A $Pt_{\sim 309}phen_{36}O_{30\pm 10}$ cluster showing a molecular weight of (7.9 ± 0.8) × 10^4 g/mol by ultracentrifugation: Schmid, G.; Morun, B.; Malm, J.-O. *Angew. Chem., Int. Ed. Engl.* **1989**, *28*, 778. (e) Recent work on $Ph_2PC_6H_4SO_3^-$-stabilized gold colloids which can be dried and then redissolved *in H_2O* show an ultracentrifugation molecular weight equal to (38 ± 8) × 10^6 g/mol. Schmid, G.; Lehnert, A. *Angew. Chem., Int. Eng. Ed.* **1989**, *28*, 780.

(30) (a) Finke, R. G. In *Polyoxometalates*; Pope, M. T., Müller, A., Eds.; Kluwer Academic: Dordrecht, The Netherlands, 1993; pp 267−280. (b) The methods and techniques developed herein have also been applied to the cyclohexene *oxidation* catalyst derived from $(Bu_4N)_5Na_3[(1,5\text{-COD})Ir{\cdot}P_2W_{15}Nb_3O_{62}]$, **1**, under O_2.[5c] Those results, which contrast dramatically the results presented herein (and thereby strengthen the conclusions of both the oxidation catalyst[5c] and the present study), strongly suggest that the oxidation catalyst derived from $(Bu_4N)_5Na_3[(1,5\text{-COD})Ir{\cdot}P_2W_{15}Nb_3O_{62}]$, **1**, is indeed, and as previously thought,[5a,b] the first authentic example of a discrete, polyoxoanion-supported, atomically dispersed homogeneous catalyst.

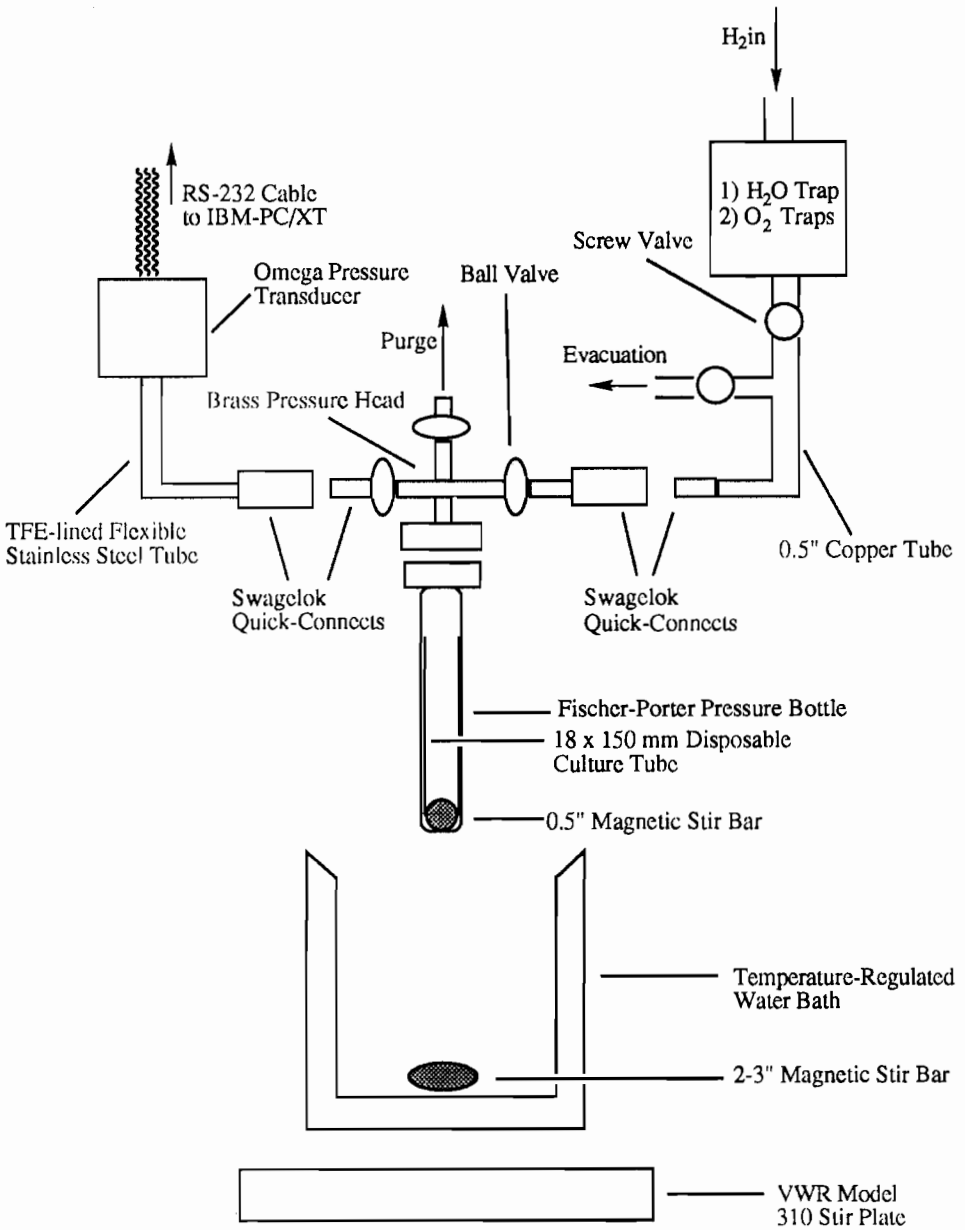

Figure 6. Schematic of the modified Fischer-Porter bottle and computer-interfaced pressure transducer system employed for the H_2 uptake and kinetic studies.

catalyst has the ability to autocatalytically hydrogenate more precatalyst **1** to catalyst). This cyclooctane production curve, Figure 7 (inset), is also key in that it means that any kinetic or phenomenological tests intended for the *catalyst* (i.e., and not the precatalyst) must be done with fully hydrogenated catalyst precursor **1** (i.e., with catalyst harvested only after ≥8 h). Failure to realize this propagated into several errors in an earlier Ph.D. thesis.[8a]

One other interesting observation is that, although ca. 0.2 equiv of (half-reduced) cyclooct*ene* is seen by GLC after ca. 1.7 h, the selectivity of the evolved catalyst is such that the final product is cyclooctane only. This selectivity is different than the selectivity to cyclooct*ene* only reported for the catalyst derived from $Ir(1,5\text{-}COD)_2^+$ in acetone,[31] but is the same as that reported for more active hydrogenation catalysts such as Crabtree's $[Ir(1,5\text{-}COD)(PPh_3)_2]PF_6$ homogeneous catalyst.[32]

A feature of the hydrogenation, Figure 7, that is misleading in that it suggests to the unwary (and given misleading literature[28b]) that the catalyst is a discrete species such as the unknown "$H_2Ir\text{-}P_2W_{15}Nb_3O_{62}^{8-}$",[10] is the ±10% reproducibility in the hydrogenation rate (i.e., in the linear part of the H_2 uptake curve). Prior to the present studies, it was widely believed[28b] that such reproducibility could not be associated with a "colloidal, heterogeneous" catalyst, a myth that the present work (plus a literature report[33]) disproves (although significant rate variations *are* typical for *traditional* metal(0) colloids[34]).

(2) The Key Mechanistic Issue: Is the True Catalyst a Discrete, "Homogeneous", Polyoxoanion-Supported Ir Complex Such as "$H_2Ir\text{-}P_2W_{15}Nb_3O_{62}^{8-}$", a "Heterogeneous" Ir_x Cluster/Colloid Catalyst, or Possibly Some New Type of

(31) Schrock, R. R.; Osborn, J. A. *J. Am. Chem. Soc.* **1971**, *93*, 3089. It is by no means obvious, given the results from our studies presented herein, that these author's catalyst, derived from $Ir(1,5\text{-}COD)_2^+$ plus H_2 and *in acetone* (the same solvent used herein), is homogenous, although the different selectivity suggests that it at least could be.

(32) (a) Crabtree, R. H. *Acc. Chem. Res.* **1979**, *12*, 331. (b) Crabtree, R. H.; Felkin, H.; Fillebeen-Khan, T.; Morris, G. E. *J. Organomet. Chem.* **1979**, *168*, 183. (c) Crabtree, R. H.; Felkin, H.; Morris, G. E. *J. Organomet. Chem.* **1977**, *141*, 205. (d) Crabtree, R. H.; Felkin, H.; Morris, G. E. *J. Chem. Soc., Chem. Commun.* **1976**, 716. (e) The precatalyst $[Ir(1,5\text{-}COD)(PPh_3)_2]PF_6$ immediately forms $[IrH_2(S)_2(PPh_3)_2]PF_6$ (S = olefin), without an induction period, when exposed to hydrogen and olefin.

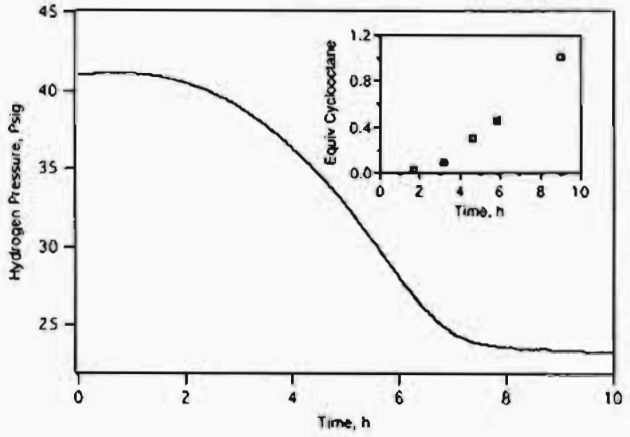

Figure 7. Reaction progress of a typical cyclohexene hydrogenation under Standard Conditions at 22 °C and in Burdick and Jackson acetone. Shown in the inset is the production of cyclooctane (detected by GLC) vs time as **1** evolves into an active catalyst. Note that the production of 1.0 equiv of cyclooctane, and thus the formation of 100% of the active catalyst, requires 8−10 h, *four times the 2 h induction period, and 1−2 h after all the cyclohexene has been hydrogenated.*

Hybrid "Homogeneous/Heterogeneous" Catalyst? (A) Isolation and Characterization of $Ir_{\sim 190-450}$ Nanoclusters Following 1000 Turnovers of Cyclohexene Hydrogenation. (i) Catalyst Isolation. Following 9 h and ca. 1000 turnovers in a Standard Conditions cyclohexene hydrogenation beginning with 20 mg of the catalyst precursor **1**, the Fischer-Porter bottle was detached from the hydrogenation line using the quick-connects and transferred back into an inert-atmosphere drybox and 3.0 mg (i.e., 15% by weight of an initial 20 mg of **1**) of a brown precipitate was isolated by filtration or gravity sedimentation followed by evacuation. (The hydrogenation of the initially 1.65 M cyclohexene to 1.65 M of the less polar cyclohexane causes the catalyst to naturally precipitate during the reaction.) This brown precipitate readily and fully dissolves in fresh (cyclohexane-free) acetone or acetonitrile to give a clear amber solution, and was shown to be an active hydrogenation catalyst (see the section below on Kinetics Studies) prior to the time-consuming studies needed to fully characterize it.

(ii) Characterization by TEM (Transmission Electron Microscopy), Electron Diffraction, Ultracentrifugation, Elemental Analysis, and IR, UV−Visible, and NMR Spectroscopies. The isolated sample of what proved to be polyoxoanion/Bu_4N^+-stabilized $Ir_{\sim 190-450}$ nanoclusters was visualized by TEM, Figure 8. The ca. 20 Å spherical dark particles were identified as Ir(0) by electron diffraction,[1] and the small, granular-appearing particles were identified as polyoxoanions. (The polyoxoanions were independently visualized in separate control experiments by employing authentic samples of polyoxoanions such as $(Bu_4N)_9P_2W_{15}Nb_3O_{62}$, its Nb—O—Nb-linked aggregate $P_4W_{30}Nb_6O_{123}^{16-}$, and, separately, the catalyst precursor $(Bu_4N)_5Na_3[(1,5\text{-COD})IrP_2W_{15}Nb_3O_{62}]$, **1**.[1]) The average size of the Ir nanoclusters, 20 ± 3 Å, was determined by counting 366 Ir nanoclusters; the resulting frequency vs nanocluster diameter histogram is shown as part of Figure 8. The 20 ± 3 Å Ir nanoclusters roughly correspond to $Ir_{\sim 190-450}$, with the average 20 Å size corresponding *approximately* to $Ir_{\sim 300}$ (the details of these calculations are available in footnote 29 of an accompanying paper[1]). Note that $Ir_{\sim 300}$ will be occasionally used hereafter *as a convenient nomenclature only* (one chosen to signify to the reader the *average* size of the nanoclusters

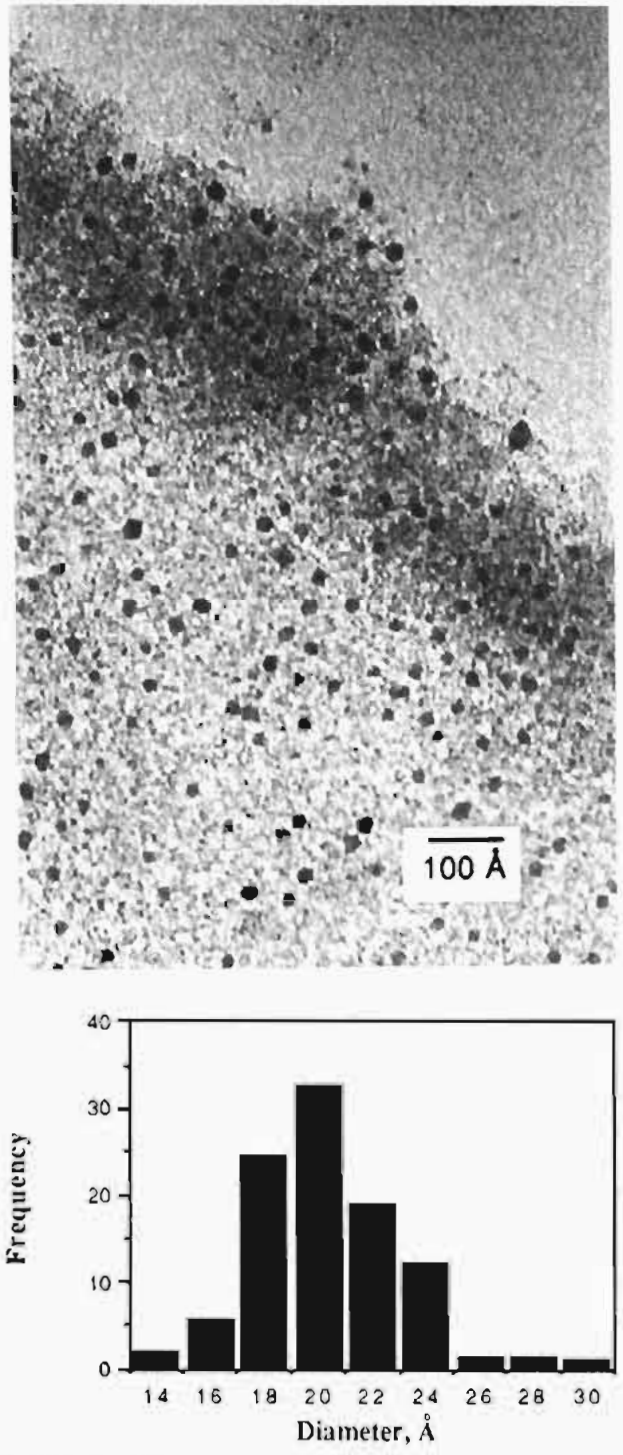

Figure 8. (A) Top: Transmission electron micrograph of the $Ir_{\sim 300}$ nanoclusters prepared from the reaction of $(Bu_4N)_5Na_3[(1,5\text{-COD})IrP_2W_{15}Nb_3O_{62}]$ with H_2 in the presence of cyclohexene. The Ir nanoclusters (dark spherical particles of ca. 20 Å) are well dispersed in the polyoxoanion matrix (small granular particles). The top and rightmost corner shows the TEM image of the carbon-film background. (B) Bottom: Histogram of the Ir nanocluster diameters. The mean diameter is 20.3 Å, with a standard deviation of 2.8 Å, from a sample population of 366.

(33) (a) Perhaps not surprisingly, the only report of ca. ±10% reproducibility in a cluster or colloid reaction is due to recent Russian work with a novel $Pd_{\sim 570\pm 30}(phen)_{63\pm 3}(OAc)_{190\pm 10}$ nanocluster.[b] (b) Vargaftik, M. N.; Moiseev, I. I.; Kochubey, D. I.; Zamaraev, K. I. *Faraday Discuss.* **1991**, *92*, 13−29 (see Table 4).

(34) (a) It is noteworthy that 5-fold rate variations are seen for the photoreduction of CO_2 catalyzed by a series of 10 different batches of the Pd colloids: Willner, I.; Mandler, D. *J. Am. Chem. Soc.* **1989**, *111*, 1330. (b) On the other hand, the distribution of clusters approximated by "$Pd_{\sim 561}phen_{60}(O_{60})(PF_6)_{60}$", and exhibiting a solution $M_t = (1.0 \pm 0.5) \times 10^5$ g/mol, shows only a 10−30% decrease for catalytic olefin oxidation following precipitation from solution.[29c] (c) Vargaftik, M. N.; Zagorodnikov, V. P.; Moiseev, I. I.; Likholobov, U. A.; Stolyarov, I. P.; Kochubey, D. I.; Chuvilin, A. L.; Zaikovsky, V. I.; Zamaraev, K. I.; Timofeeva, G. I. *J. Chem. Soc., Chem. Commun.* **1985**, 937. (d) See also ref 29c.

present); *this nomenclature is not meant to imply that a monodispersed, exactly Ir_{300} nanocluster is the only species present.* In addition, four types of TEM control experiments were also done to ensure that the TEMs reported (i) are representative of the bulk sample, (ii) are repeatable, (iii) are unchanged by either exposure time or electron beam voltage, and (iv) are not dependent on the sample preparation or spraying method (i.e., spraying under air or N_2 onto the carbon-coated Cu TEM grid).[1]

Ultracentrifugation solution MW (molecular weight) analyses were used to confirm that the $Ir_{\sim 300}$polyoxoanion nanoclusters also persist in solution. The results show a weight-average molecular weight, $\bar{M}_r$, of 86 000 ± 40 000 (Figure A, supplemental material) that is within error of, but somewhat larger than, the expected median of the calculated MW range of 36 500−86 500 for *naked* $Ir_{\sim 190\text{-}450}$. This slightly larger $\bar{M}_r$ suggests that, even after ultracentrifugation, *the $Ir_{\sim 190-450}$ nanoclusters retain some of their associated polyoxoanions*, thereby raising the observed MW. Electrophoresis experiments on the closely related $Ir_{\sim 900}$ nanoclusters show that they are negatively charged,[1] results which independently confirm that the polyoxoanions are intimately associated with the $Ir_{\sim 300}$ and $Ir_{\sim 900}$ nanoclusters.

Interestingly, in a separate ultracentrifugation experiment it was found that the clear amber solution (obtained by dissolving the brown $Ir_{\sim 300}$polyoxoanion/Bu_4N^+ precipitate in either acetone or CH_3CN in the drybox) could be separated into primarily its lighter polyoxoanion component and much heavier $Ir_{\sim 300}$polyoxoanion nanoclusters. This separation was accomplished simply by rotation of the amber solution in an ultracentrifugation cell at 20 000 rpm for less than 10 min. As detailed further in the Experimental Section, this led to a colorless supernatant containing the polyoxoanion (*vide infra*) and a dark-brown deposit of the $Ir_{\sim 300}$polyoxoanion nanoclusters. *Simple shaking of the solution redissolves all of dark-brown solid and reestablishes the clear, amber solution.* This result strongly suggests (i) that some polyoxoanions are still retained by centrifuged $Ir_{\sim 300}$ nanoclusters (preventing their aggregation) and (ii) that the number of polyoxoanions (and Bu_4N^+) associated with the $Ir_{\sim 300}$ nanoclusters is a primary determinant in establishing the solubility of the $Ir_{\sim 300}$ nanoclusters.

To confirm that the clear supernatant contained polyoxoanions, a separate MW experiment (at a 20 000 rpm ultracentrifugation rotation speed appropriate for the much lighter polyoxoanion) was performed to obtain the molecular weight of the polyoxoanion component of the $Ir_{\sim 300}$polyoxoanion nanoclusters. The result, a MW = 10 800 ± 2000 (Figure B, supplementary material), establishes that the predominant polyoxoanion present in solution is actually the Nb—O—Nb bridged aggregate, $P_4W_{30}Nb_6O_{123}^{16-}$, calculated FW (formula weight) = 8165. This is, however, as expected, since the same Nb—O—Nb-bridged polyoxoanion was also found in the $Ir_{\sim 900}$polyoxoanion nanoclusters.[1] The presence of polyoxoanions in the isolated brown precipitate was also confirmed using IR spectroscopy.

Elemental analysis was obtained (by Pascher, with handling under N_2) on a sample of the isolated brown Ir nanoclusters. The results, when combined with a solution MW of ca. 86 000, establish an *average* molecular formula of $[Ir(0)_9(P_4W_{30}Nb_6O_{123}^{16-})](Bu_4N)_9Na_7$ or, scaling up to the average $Ir_{\sim 300}$ size indicated by the TEM and solution MW measurement, $[Ir(0)_{\sim 300}(P_4W_{30}Nb_6O_{123}^{16-})_{\sim 33}](Bu_4N)_{\sim 300}Na_{\sim 233}$. UV−visible spectroscopy was also used to examine an amber, acetone solution of the isolated Ir nanoclusters. As also seen for the larger $Ir_{\sim 900}$ nanoclusters,[1] the UV−visible displays no maxima but, instead, exhibits a trailing decrease in adsorption with increasing wavelength due to light-scattering (i.e., plasmon resonance)[35a,b] by the Ir nanoclusters (Figure C, supplementary material). Finally, the brown precipitate was also characterized by ^1H NMR spectroscopy. As expected on the basis of the findings for the larger $Ir_{\sim 900}$ nanoclusters, no Ir—hydride peak was detected (and, confirming this, no Ir—H IR resonance is seen; see the Experimental Section). The results for $Ir_{\sim 300}$ parallel the results for the $Ir_{\sim 900}$ nanoclusters,[1] with both sets of data demonstrating that no NMR[35c] (or IR) detectable Ir—H hydrides are present.

(B) Characterization of the (Same) $Ir_{\sim 300}$ Nanoclusters in the Filtrate Following a Standard Conditions Cyclohexene Hydrogenation. The clear, light-yellow filtrate obtained from the reaction solution (i.e., the filtrate following removal of the ca. 15% of brown precipitate in an inert-atmosphere drybox) was also examined by TEM and other physical methods (including IR and NMR, which again confirmed the presence of polyoxoanions and the absence of Ir—H hydrides). The key finding is that significantly fewer (but still the same) ca. 20 Å $Ir_{\sim 300}$ nanoclusters are seen as were also seen in the brown precipitate (the TEM, and additional characterization of the light-yellow filtrate, are available elsewhere[1]). This result agrees well with the kinetic studies, presented next, showing that most of the catalytic activity resides in the isolated brown precipitate rather than in solution. When taken together, the TEM and the kinetic results demonstrate that the catalytic activity exhibits a positive correlation with the number of Ir nanoclusters present (*vide infra*).

(C) Demonstration That the Isolated $Ir_{\sim 190-450}$ Nanoclusters Are in Fact the True Catalysts. (i) Kinetic Studies. The kinetic evidence that the isolated $Ir_{\sim 190-450}$polyoxoanion nanoclusters are indeed the true catalyst materials is sixfold and compelling. First, a sample of 3.0 mg of the isolated brown precipitate of $Ir_{\sim 190-450}$polyoxoanion nanoclusters (i.e., 15% by weight of the initial 20 mg of **1** used to produce the precipitate) was found to catalyze cyclohexene hydrogenation *without* an induction period and with an initial rate of 0.77 mmol of H_2/h, which is 70% of the maximum rate ($\{-d[H_2]/dt\}_{apparent}$ = 1.1 mmol of H_2/h) seen in the Standard Conditions hydrogenation experiment, Figure 9. This establishes that the isolated $Ir_{\sim 190-450}$ nanoclusters posses kinetic competence to be the true catalyst. Second, and as previously mentioned, the burst of catalytic activity after the induction period can be fit quantitatively *only* by autocatalysis[1,10] (eq 5 in Scheme 1; *vide infra*).

Third, adding only 1.7×10^{-4} equiv (per equiv of **1**) of the $Ir_{\sim 190-450}$polyoxoanion nanoclusters to the start of an otherwise Standard Conditions cyclohexene hydrogenation shortens the induction period by 50% and leads to the same rate ($-d[H_2]/dt_{apparent}$ = 1.1 mmol of H_2/h) that is seen beginning with **1**, Figure 10. Similarly, the addition of 0.04 equiv of the nanocluster-forming solvate[1] $Ir(1,5\text{-COD})(acetone)_2^+$ leads to 38% shortening of the induction period, plus a limiting rate of $-d[H_2]/dt_{apparent}$ = 1.1 mmol of H_2/h, Figure 10. *These results confirm that the formation of the $Ir_{\sim 300}$ nanoclusters accounts for both the induction period and, then, the subsequent autocatalysis.*[1] The proposed mechanistic steps leading to $Ir_{\sim 300}$ formation and autocatalysis are shown in Scheme 1 (steps that are also supported by several lines of evidence presented in a recent paper[1]).

(35) (a) Perez-Benito, J. F.; Arias, C. *Int. J. Chem. Kinet.* **1991**, *23*, 717. (b) The UV−visible spectrum of our $Ir_{\sim 190-450}$ nanoclusters parallels closely that provided for a water-soluble Ir colloid given in a recent tabulation containing the UV−visible spectra of 52 metal colloids: Creighton, J. A.; Eadon, D. G. *J. Chem. Soc., Faraday Trans.* **1991**, *87*, 3881. (c) Vargaftik and co-workers[29c] have shown that $Pd(0)_x$—H nanocluster hydrides display a very broad peak in the ^1H NMR, a broad peak observable only in a broad-band (250 KHz) spectrum.

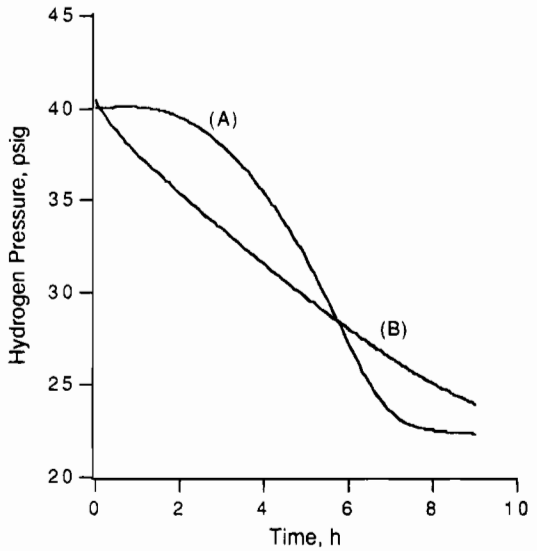

Figure 9. Comparison of cyclohexene hydrogenation: (a) starting with 20.0 mg of **1** as in a typical, Standard Conditions cyclohexene catalytic hydrogenation; (b) starting with 3.0 mg (i.e. ca. 15% of the starting **1** by weight) of the brown $Ir_{\sim 190-450}$-polyoxoanion precipitate. The constant rate, $\{-d[H_2]/dt\}_{apparent}$, after the induction period in (a) is 1.1 mmol of H_2/h, while the initial rate, $\{-d[H_2]/dt\}_{initial}$, in (b) is 0.77 mmol of H_2/h. In other words, this experiment shows that 15% by weight of the isolated $Ir_{\sim 190-450}$-polyoxoanion nanocluster catalyst can account for 70% of the hydrogenation rate seen when beginning with **1**.

Scheme 1. Proposed Mechanism for the Formation (Nucleation and Growth Steps) of Polyoxoanion-Stabilized $Ir(0)_{n\rightarrow m}$ Nanoclusters[1]

$$[(1,5\text{-COD})Ir{\cdot}P_2W_{15}Nb_3O_{62}]^{8-} + 2\,S\ (S = \text{acetone}) \underset{}{\overset{K_{eq} << 1}{\rightleftharpoons}} Ir(COD)S_2^{+} + P_2W_{15}Nb_3O_{62}^{9-} \quad (2)$$

(**1**, 1,5-COD = cyclooctadiene)

$$Ir(1,5\text{-COD})S_2^{+} + 2.5\ H_2 \longrightarrow \bigcirc + Ir(0) + H^{+} \quad (3)$$

$$n \rightarrow m\ Ir(0) \xrightarrow{\text{nucleation}} Ir(0)_{n\rightarrow m} \quad (4)$$

$$1 + 2.5\ H_2 + [Ir(0)]_{n\rightarrow m} \xrightarrow[\text{(on the } [Ir(0)]_{n\rightarrow m} \text{ nanocluster's surface)}]{\text{autocatalysis}} \bigcirc + [Ir(0)]_{(n\rightarrow m)+1} + H^{+} \quad (5)$$

Fourth, the (only) Ir product following autocatalysis and after ca. 1000 catalyst cycles was isolated and shown to be $Ir_{\sim 190-450}$-polyoxoanion nanoclusters. The kinetic evidence presented so far, when combined with the finding that the $Ir_{\sim 300}$-polyoxoanion nanoclusters are the only detectable Ir species after ca. 1000 catalyst cycles, provides seemingly incontrovertible evidence that the $Ir_{\sim 190-450}$-polyoxoanion nanoclusters are the true catalysts.

A fifth type of kinetic evidence compares the TON (turnover number) of both the *in situ* generated nanocluster catalyst and the isolated $Ir_{\sim 190-450}$ nanoclusters to well-established Ir(0) heterogeneous catalysts. As Table 1 details, the rates of the nanocluster and authentic Ir(0) catalysts are all essentially the same within experimental error, TON = 3000 ± 1000 turnovers/h, demonstrating that the true catalyst has the reactivity expected for Ir(0). Moreover, how the TON for the $Ir_{\sim 190-450}$ nanoclusters was calculated is an additional piece of evidence implicating the $Ir_{\sim 300}$ nanoclusters as the true catalysts. Specifically, the TON = 3200 ± 1400 turnovers/h for $Ir_{\sim 190-450}$ requires, as input, PPh_3 poisoning data (*vide infra*; see Table 2, where 0.2 equiv of PPh_3 completely poison the catalyst). Alternatively,

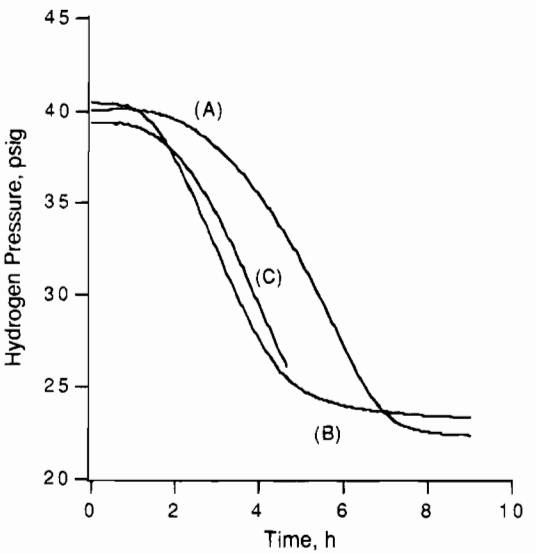

Figure 10. Effect of the addition of $Ir_{\sim 190-450}$ nanoclusters or Ir(1,5-COD)(acetone)$_2^+$ to the cyclohexene hydrogenation reaction starting with **1**. (A) normal "Standard Conditions" hydrogenation curve for comparison; (B) with the addition of only 1.7×10^{-4} equiv of $Ir_{\sim 190-450}$ (per equiv of **1**); (C) with the addition of 0.04 equiv of Ir(1,5-COD)-(acetone)$_2^+$. This experiment demonstrates that even 1.7×10^{-4} equiv of added $Ir_{\sim 190-450}$ nanoclusters shortened the induction period by 50% (and is, therefore, consistent with and strongly supportive of the hypothesis that the induction period is due to **1** + H_2 slowly forming $Ir_{\sim 190-450}$ nanoclusters).

a second estimate of the fraction of total Ir(0) atoms that is available and active on the $Ir_{\sim 300}$ nanocluster's surface is ca. 52%, since an idealized Ir_{309} "full-shell" cluster[36] would have exactly 52% of its metal atoms on the surface. *The key point here is that such a fraction is a (geometric) feature very hard to achieve in any other conceivable (i.e., noncluster) Ir(0) catalyst* (and assuming that the fraction of Ir(0) that is inactive is not "poisoned" in some other, nongeometrical way.) The Experimental Section, under Hydrogenations, Table 2, and elsewhere[36] contain further details regarding the estimate of the fraction of active Ir(0), 0.2 ≤ active Ir(0) ≤ 0.5, for the interested reader.

The $Ir_{\sim 190-450}$ average TON of ca. 3000 turnovers/h is an important finding in another respect: *the reactivity of the polyoxoanion-stabilized $Ir_{\sim 190-450}$ nanoclusters is as high as any Ir(0) catalyst tested.* This includes Exxon's[37] 80% dispersed 1% Ir(0) on Al_2O_3, Table 1, the most highly dispersed heterogeneous Ir(0) catalyst that we could find, a material that is one of the best characterized Ir(0) heterogeneous catalysts as well.

A sixth type of kinetic evidence was obtained by examining the effect of two different polyoxoanions on the hydrogenation reaction's induction period and rate. The well-characterized, $SiW_9Nb_3O_{40}^{7-}$-supported system, $(Bu_4N)_4Na_2[(1,5\text{-COD})IrSiW_9Nb_3O_{40}]$, **2**,[38] was employed as the precatalyst for a comparison to the $P_2W_{15}Nb_3O_{62}^{9-}$-supported system, **1**. It was found that under the same conditions, the hydrogenation reaction starting with **2** proceeds with a slightly longer induction period of 2.5 ± 0.3 h but otherwise is very similar to that beginning with **1**,

(36) Lead references include: (a) Teo, B. K.; Sloane, N. J. A. *Inorg. Chem.* **1985**, *24*, 4545. (b) Schmid, G. *Struct. Bonding* **1985**, *62*, 51–85. (c) Schmid, G.; Klein, N.; Morun, B.; Lehnert, A.; Malm, J. O. *Pure Appl. Chem.* **1990**, *62*, 1175–7. (d) See also ref 15.

(37) (a) McVicker, G. B.; Baker, R. T. K.; Garten, R. L.; Kugler, E. L. *J. Catal.* **1980**, *65*, 207. (b) Key physical data for this well-characterized catalyst: 1.04% by weight Ir (prepared by incipient wetness impregnation of η-alumina with aqueous H_2IrCl_6, followed by calcining at 270 °C for 4.0 h under dry air); BET = 154 m^2/g; H/Ir = 2/0 (total), 1.6 (irreversible); CO/Ir = 1.5.

(38) Lin, Y.; Nomiya, K.; Finke, R. G. *Inorg. Chem.* **1993**, *32*, 6040.

Table 1. Activity Comparison of Heterogeneous Iridium Catalysts vs Polyoxoanion-Supported Iridium Precatalysts[a]

(pre)catalyst	turnovers/h (per exposed Ir(0))	tot. turnovers (demonstrated)
(1,5-COD)Ir·$P_2W_{15}Nb_3O_{62}^{8-}$ (**1**)	3200 ± 1000[b] (1100 ± 500)[b,d]	18 000[c]
(1,5-COD)Ir·$SiW_9Nb_3O_{40}^{6-}$ (**2**)	3200 ± 1000[b] (1100 ± 500)[b,d]	4 000[c]
Exxon's 80% dispersed Ir/η-Al_2O_3	1740 ± 250[c,e]	20 000[c,e]
commercial 7.9% dispersed Ir/γ-Al_2O_3	3950 ± 1000[c,e]	410 000[c,e]
$[Ir^0]_n$ (from $[Ir(1,5\text{-COD})(CH_3CN)_2]BF_4$ plus H_2)	3900 ± 600,[c,e] 775 ± 725[f]	51 600[c,e]
$(Bu_4N^+)_9(P_2W_{15}Nb_3O_{62})$ (zero Ir control reaction)	0	0

[a] The Standard Conditions for hydrogenation were used (i.e., 1.65 M purified cyclohexene and 40 psig H_2) except that *Baker acetone distilled from K_2CO_3 was used as solvent* in these early experiments (unless noted otherwise). [b] Calculated in this case from TON = $\{-d[H_2]/dt_{apparent}$ (in mmol of H_2/h)$\}/[0.2$ (*or* 0.5) $\times$ 0.0035 mmol catalyst], where 0.2 (or 0.5) is the correction for the number of Ir(0) atoms that are active by PPh_3 poisoning studies (or are calculated to be present on the surface; see the Experimental Section on "Hydrogenations" for further details). The error bars in $-d[H_2]/dt_{apparent}$ are small (i.e., typically $\leq 10\%$, $-d[H_2]/dt_{apparent} = 1.1 \pm 0.1$ for instance, so that the major error is in the estimate of the 0.2−0.5 fraction of the total Ir(0) that is active. [c] These data are taken from D. Edlund's Ph.D. thesis;[7a] note that the acetone employed was dried over 3 Å mol sieves. [d] These entries used Burdick & Jackson acetone; see Table 2 for additional details. [e] All runs are from a single batch of material; turnover numbers are corrected for the number of available and active Ir(0) (see the Experimental Section). [f] Runs from multiple batches; turnover numbers are deliberately not corrected for the Ir(0) surface area; hence, the error bars reflect the ca. 100% variability in the surface area of the precipitates.

reaching the identical linear rate as seen for **1**, $\{-d[H_2]/dt\}_{apparent} = 1.1 \pm 0.1$, Figure 11 and entry 1 of Table 2. This nearly identical reactivity requires closely similar active sites in the two catalysts, and TEM confirms that this is true, with **2** yielding 23 ± 3 Å, $Ir_{\sim 265-640}$ (i.e., $Ir_{\sim 400}$) nanoclusters (as reported elsewhere[1]). The similarity in the active sites of the catalyst derived from **1** and **2** suggests that the *different* polyoxoanions are either bound rather loosely to the $Ir_{\sim 190-450}$ nanoclusters or are, on the average, bound to the $Ir_{\sim 190-450}$ nanocluster somewhat away from the catalytically active sites.

In summary, the six lines of kinetic evidence presented provide a compelling case that the isolable $Ir_{\sim 190-450}$ nanoclusters are the true catalysts.[39]

(3) Phenomenological Homogeneous vs Heterogeneous Catalysis Tests. The main interest here is to see how a well-characterized nanocluster behaves in several of these often classical, but sometimes misleading, tests. The results of each test are summarized in Table 2 (along with solvent dependence, H_2O dependence, and other data that will also be discussed in turn).

(A) Catalyst Isolation (Evacuation to Dryness) and then Reuse Experiments. To further characterize the isolated catalyst kinetically, three cycles of evaporation to dryness and then restarting a new cyclohexene hydrogenation with fresh acetone and cyclohexene were examined. These experiments are of interest since classical colloids or clusters can agglomerate under such treatment.[40] The results are presented graphically in Figure 12 and are tabulated as entry 2 of Table 2; they show that the initial rate for fully formed catalyst (i.e., after the first evaporation/reuse cycle) is $\{-d[H_2]/dt\}_{initial} = 1.7$ mmol of H_2/h, which is 55% higher than the 1.1 mmol of H_2/h seen from **1** to start, but the initial rate then decreases by 59% in the second evaporation/reuse cycle to 1.0 mmol of H_2/h, Figure 12. The $Ir_{\sim 190-450}$ nanoclusters have, apparently, been partially deactivated (presumably by agglomeration) by two cycles of evaporation to dryness. However, *no bulk Ir metal particles are ever observed in these experiments*, providing further evidence that the isolable $Ir_{\sim 190-450}$ nanoclusters are still remarkably stable in comparison to traditional Ir colloids.

(B) PPh_3 Poisoning Studies. The prediction accompanying the identification of $Ir_{\sim 190-450}$ nanoclusters as the active catalyst is that $\leq 50\%$ of the Ir originally present in the precatalyst **1** will be on the surface and thus available for PPh_3 binding (i.e., recall the calculation noted above indicating that 52% of the Ir(0) metal atoms are on the surface of an idealized, Ir_{309} "full-shell" cluster;[36] note that this 52% is less than or equal to the maximum number of *bulky* PPh_3 groups that should be able to bind). Consistent with this prediction, the presence of 0.2 equiv of PPh_3 was found to completely suppress cyclohexene hydrogenation, Figure 13 and entry 3 of Table 2. This result cannot be explained by a homogeneous Ir catalyst such as "L_2Ir·$P_2W_{15}Nb_3O_{62}^{8-}$",[41] which would be expected to take ≥ 1 equiv, and probably exactly 2.0 equiv, of PPh_3 to poison its "L_2-Ir-polyoxoanion" active site. Rigorously, this result requires only that $\leq 20\%$ of the Ir(0) present be available for PPh_3 binding (and, for this reason, further poisoning studies with different size and types of ligands are planned).

(C) Hg Poisoning Tests. Hg is a well-known[42] poison for heterogeneous catalysts due to amalgam formation with the metal catalyst, a fact that was first exploited by Whitesides and co-workers.[17,21] The Hg test is presently one of the most popular and easiest to use "homogeneous vs heterogeneous" tests; hence, it was of interest to examine this test carefully[43] and in some detail with both the well-characterized precatalyst **1** and with the $Ir_{\sim 300}$ nanoclusters.

(39) (a) The case is fortified by the "Method of Holmes", in that there is no other reasonable possibility for the catalyst besides the $Ir_{\sim 190-450}$ nanoclusters (or their fragments, which *are also nanoclusters*), at least that we can see (nor that the reviewers were able to offer) and *which can also account for all the evidence presented.* (b) A statement of the Method of Holmes, a method of exclusion that is essentially one version of the scientific method (and, therefore, has been referenced in the chemical literature[39d,e,g]) is as follows: "When you have eliminated the impossible, whatever remains, however improbable, must be the truth." Note, of course, that we *do not* mean to imply that we have "proven" (or that one can "prove") a mechanism! (c) S. Holmes, as quoted by J. J. Watson: Doyle, A. C. The Adventure of the Bruce-Partington Plans. *The Complete Sherlock Holmes*; Garden City Publishing: Garden City, NY, 1930; p 1089. See also pp 118, 360, and 1192, for slightly different quotations. (d) Dickerson, R. E.; Wheatley, P. J.; Howell, P. A.; Lipscomb, W. J.; Schaeffer, R. *J. Chem. Phys.* **1956**, *25*, 606. (e) Noyes, R. *J. Am. Chem. Soc.* **1968**, *90*, 668. (f) It is a special pleasure to acknowledge Professor Dick Noyes for his assistance in locating the references cited. (g) Cotton, F. A. *J. Organomet. Chem.* **1975**, *100*, 29.

(40) In the absence of appropriate protecting agents, metal colloids or clusters originally dispersed in a solvent agglomerate to give bulk metal when evacuated to dryness due to Van der Waals attractions. For example, a Pd colloid dispersed in acetone [i.e., $(Pd)_n(CH_3COCH_3)_y$] gives a metal-like Pd film upon solvent evaporation: Cardenas-Trivino, G.; Klabunde, K. J.; Dale, E. B. *Langmuir* **1987**, *3*, 986.

(41) The failure to report this key, ≤ 1 equiv of PPh_3 poisoning experiment in an earlier Ph.D. thesis (i.e., despite the fact that the experiment was in fact done as a laboratory notebook verifies),[8] presumably because it did not fit the researcher's bias[8a] that the catalyst was a "L_2Ir·$P_2W_{15}Nb_3O_{62}^{8-}$" species,[8b] is a serious scientific error (one treated in more detail elsewhere[9]). As Figure 3 and the approach herein emphasize, the correct mechanism and catalyst description will of course explain *all* the data.

(42) Paal, C.; Hartmann, W. *Ber. Dtsch. Chem. Ges.* **1918**, *51*, 711.

(43) Of special interest is whether or not the Hg reacts with the precatalyst **1** and thus whether or not this test was really "useless for the present example" as had been tentatively concluded earlier (and incorrectly, as it turns out).[8,10a]

Table 2. Variables Affecting the $Ir_{\sim 300}$ Nanocluster Hydrogenation of Cyclohexene under Otherwise Standard Conditions[a]

	induction period (h)	hydrogenation rate[b]	comments
		Polyoxoanion Effect	
(1) $P_2W_{15}Nb_3O_{62}^{9-}$ (i.e., **1** as precatalyst)	2.0 ± 0.2	1.1 ± 0.1	error bars were obtained from 10 experiments with **1** and from 3 experiments with **2**
(2) $SiW_9Nb_3O_{40}^{7-}$ (i.e., **2** as precatalyst)	2.5 ± 0.3	1.1 ± 0.1	
		Three Cycles of Catalyst Isolation and Reuse	
cycle 1	2.0	1.0	In cycle 1 (the catalyst generation cycle) the reaction was stopped after 95% H_2 uptake. In cycles 2 and 3, the active $Ir_{\sim 300}$ catalyst derived from cycle 1 was used instead (without isolation and in the same reaction vessel).
cycle 2	0	1.7 (initial rate)	
cycle 3	0	1.0 (initial rate)	
		PPh_3 Poisoning Experiment	
expt 1 (a control with no PPh_3 added)	0	1.5 (initial rate)	In both reactions, the active $Ir_{\sim 300}$ catalyst (the isolated brown ppt from **1**) was used instead of the precatalyst, **1**.
expt 2, with 0.2 equiv of PPh_3/equiv of Ir added	no activity	no activity	
		Hg Test Experiments (and Controls)	
expt 1	4.0	1.2	In experiment 1, the precatalyst **1** is stirred with Hg which is then *removed* from the reaction solution. In experiment 2, Hg *is present* in the reaction solution throughout the experiment
expt 2	no activity	no activity	
		Acetone Solvent (Source and Treatment)	
(1) Burdick & Jackson acetone (0.10 M H_2O)	2.0 ± 0.2	1.1 ± 0.1	85 equiv of H_2O/equiv **1**
(2) Baker acetone (0.15 M H_2O)	1.4 ± 0.2	1.2 ± 0.1	128 equiv of H_2O/equiv **1**
(3) Baker acetone distilled from K_2CO_3 (0.42 M H_2O)	1.5 ± 0.2	3.3 ± 0.3	357 equiv of H_2O/equiv **1**
(4) acetone from (3) above but redistilled from $CaSO_4$	2.5	1.2	(Error bars are obtained from more than 5 experiments in each example.)
		Effects of H_2O	
80 equiv of H_2O	2.0	1.1	In the cases of ≥1660 (to 5600) equiv of added H_2O, a bulk and insoluble bulk Ir(0) ppt is observed.
1180 equiv of H_2O	0.9	1.6	
1660 equiv of H_2O	0.5	3.2	
5600 equiv of H_2O	0	5.4 (initial rate)	
		Effects of HOAc (and OAc^- as a Control)	
0 equiv	2.0	1.1	Even in the case of 61 equiv of added HOAc, no bulk Ir(0) precipitate is observed
4.3 equiv	0.5	1.8	
61 equiv	0.2	6.4	
90 equiv of $Bu_4N^+OAc^-$ (control expt)	2.0 (no effect)	1.1 (no effect)	
		Other Solvents[c]	
CH_3CN	0	(See Table 1 for a chemisorption-corrected value for the *ppt formed*)	Bulk Ir(0) ppt forms within 1 h
CH_2Cl_2	no activity	no activity	no activity seen even after 38 h
$C_2H_4Cl_2$	ca. 7	0.5	roughly half the activity as seen in acetone

[a] Standard Conditions as defined in the Experimental Section, including starting with 1.2 mM $(Bu_4N)_5Na_3[(1,5\text{-COD})IrP_2W_{15}Nb_3O_{62}]$, **1**, 1.65 M cyclohexene, 22 °C, and 40 psig H_2 and using Burdick & Jackson acetone. [b] $\{-d[H_2]/dt\}_{apparent}$ or, if indicated, the initial rate, $\{-d[H_2]/dt\}_{initial}$ (mmol of H_2/h). [c] Studies of other solvents (DMF, DMSO, nitromethane, propylene carbonate) are available as well.[8a]

Four types of experiments were done, leading to consistent and unequivocal results (entry 4, Table 2 summarizes the results of the two main experiments; two additional, confirming experiments are available to the interested reader in the Experimental Section). The key results are as follows: (i) A yellow solution of precatalyst **1** does in fact change color to orange and some of the Hg does acquire a gray film, *but* if the Hg is then removed, **1** still evolves into a fully active catalyst (although the trace Hg that remains causes the induction period to go from a normal 2 to 4 h). (ii) However, if Hg is left in with **1** no activity evolves. (iii) Isolated fully active $Ir_{\sim 300}$ catalyst is *completely* deactivated in the presence of Hg, a result consistent with experiment number (ii).

These Hg tests experiments offer yet additional support to postulate that the $Ir_{\sim 300}$ nanoclusters are the true catalyst. In addition, the fact that even trace Hg increases the induction period from 2 to 4 h *offers strong, independent evidence fortifying the hypothesis that nucleation to active Ir nanoclusters is the source of the induction period and subsequent autocatalysis*. Last, these results provide additional evidence[17,19,21,25] that the Hg test is one of the fastest and more reliable tests for distinguishing homogeneous from heterogeneous catalysts (as long as the necessary control experiments are also performed).

(D) Different Sources and Pretreatment of Acetone and the Effects of Added H_2O and H^+. One of the early, unusual and initially puzzling features in these studies was the finding that the cyclohexene hydrogenation rate was reproducible within ±10% in Baker acetone, "purified" by distillation from K_2CO_3, even in the hands of different researchers, but that the use of Burdick and Jackson acetone gave a 300% slower rate, one that is, however, *also reproducible to ≤±10%!*, Table 2 and Figure 14. The different water contents of the different samples of acetone was suspected as a contributing agent, and a water-sensitive dye method[44] was used to determine accurately the H_2O content of the various solvents listed in Table 2. Experiments adding increasing amounts of H_2O to the ("driest", 0.1

(44) Langhals, H. *Anal. Lett.* **1990**, *23*, 2243.

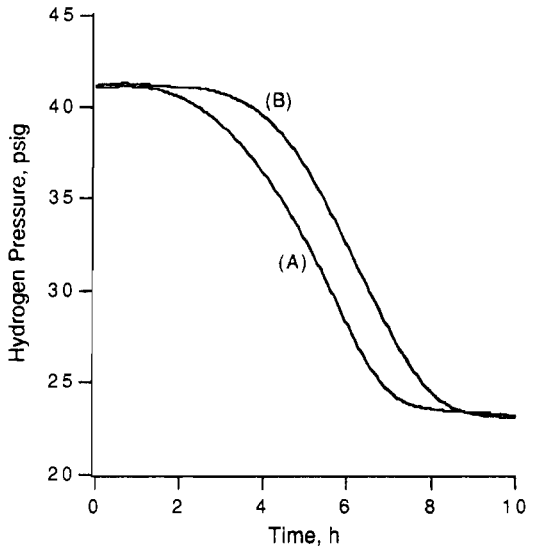

Figure 11. Comparison of the cyclohexene hydrogenation using (a) $(Bu_4N)_5Na_3[(1,5\text{-COD})Ir{\cdot}P_2W_{15}Nb_3O_{62}]$, **1**, and (b) $(Bu_4N)_4Na_2[(1,5\text{-COD})Ir{\cdot}SiW_9Nb_3O_{40}]$, **2**, as the catalyst precursor. Note that, other than the slightly longer induction period, the curves are very similar indicating that **1** and **2** give quite similar catalysts despite being composed of rigorously different (but otherwise quite similar, basic and Nb—O containing) polyoxoanions. Numerical data from this experiment are summarized in Table 2.

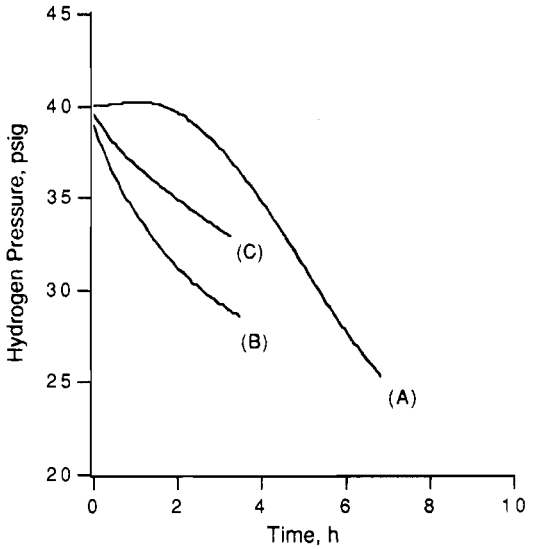

Figure 12. Hydrogenation curves for three cycles of cyclohexene hydrogenation: (A) first cycle starting with **1** under Standard Conditions; (B) second cycle starting with the material from the first cycle after evaporating it to dryness under vacuum at room temperature; (C) third cycle starting with the material from the second cycle after its evaporation to dryness. See Table 2 for the numerical results from these experiments.

M H_2O containing) Burdick and Jackson acetone, followed by cyclohexene hydrogenation under otherwise Standard Conditions, revealed that increasing amounts of H_2O significantly shorten the induction period and increase the rate, by up to ca. 3-fold at 1660 equiv of H_2O vs 1 equiv of starting **1**, Figure 15. [However, at or beyond 1660 equiv (1.9 M) H_2O, bulk Ir(0) metal precipitates.] An especially convincing experiment, demonstrating that the acetone H_2O content and pretreatment are key, is the experiment listed in Table 2, where the 3-fold faster rate in Baker acetone distilled from K_2CO_3 is reverted to *a 3-fold slower, typical 1.2 mmol of H_2/h rate* following drying and distillation of the Baker acetone from the recommended drying agent,[45] $CaSO_4$.

However, careful and quantitative experimentation revealed

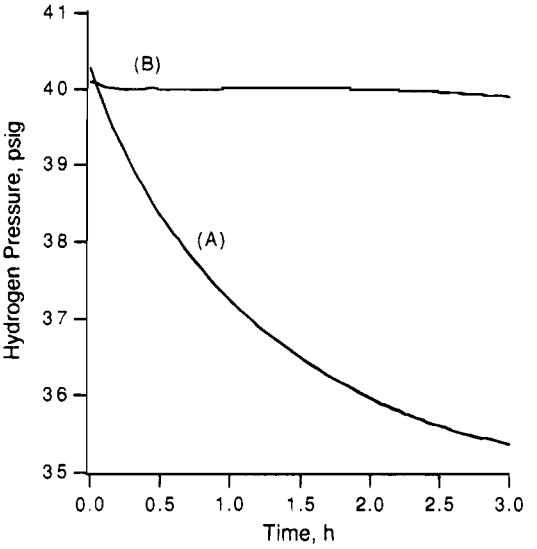

Figure 13. The effect of PPh_3 on the cyclohexene hydrogenation starting with the $Ir_{\sim 190-450}$ nanoclusters derived from **1**: (A) active catalyst; (B) active catalyst plus 0.2 equiv of PPh_3, which completely inhibited the cyclohexene hydrogenation.

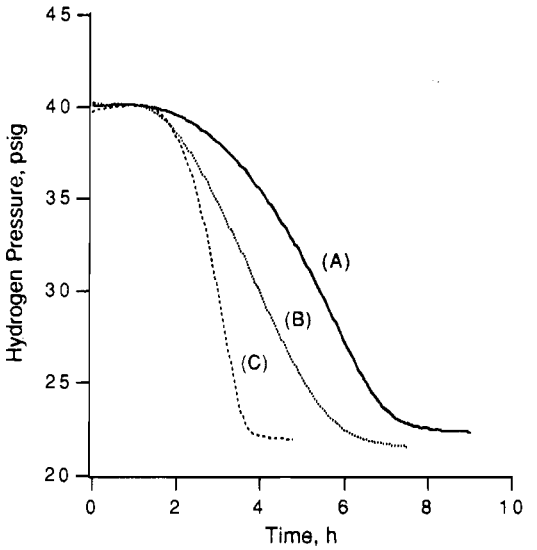

Figure 14. Cyclohexene hydrogenation starting with **1** but in different batches of acetone: (A) Burdick & Jackson's acetone (containing 0.2% water, i.e., 0.10 M H_2O, or 85 equiv vs the 1.18 mM **1**); (B) Baker's acetone (containing 0.3% water, i.e., 0.15 M H_2O, or 128 equiv vs **1**); (C) Baker's acetone, distilled from K_2CO_3 (containing 0.42 M H_2O or 357 equiv vs **1** and also containing another unidentified, possibly aldol-condensation product derived from acetone).[46] See the Experimental for further details.

that adding even 1180 equiv of H_2O (i.e., 3.3 times the 357 equiv present in Baker acetone) results in only 45% of the observed 300% rate increase in $\{-d[H_2]/dt\}_{apparent}$ (i.e., the rate increase seen on going from Burdick & Jackson to Baker acetone distilled from K_2CO_3, Table 2). Hence, some other, presumably K_2CO_3-induced aldol-condensation products from acetone (more than 15 of which are known[46]) present in the "K_2CO_3 purified" Baker acetone must be important in giving the observed rate enhancement, and we are still tracking down this detail. (Four impurities have been detected by GC-mass spectroscopy, but we have not yet unequivocally identified them structurally; the interested reader is referred to the Experimental Section for additional information.)

(45) Coetzee, J. F.; Chang, T.-H. *Pure Appl. Chem.* **1986**, *58*, 1535.
(46) Salvapati and co-workers have shown that bases such as K_2CO_3 can catalyze aldol condensations of acetone to produce water plus more than 15 products: Salvapati, G. S.; Ramanamurty, K. V.; Janardanarao, M. *J. Mol. Catal.* **1989**, *54*, 9.

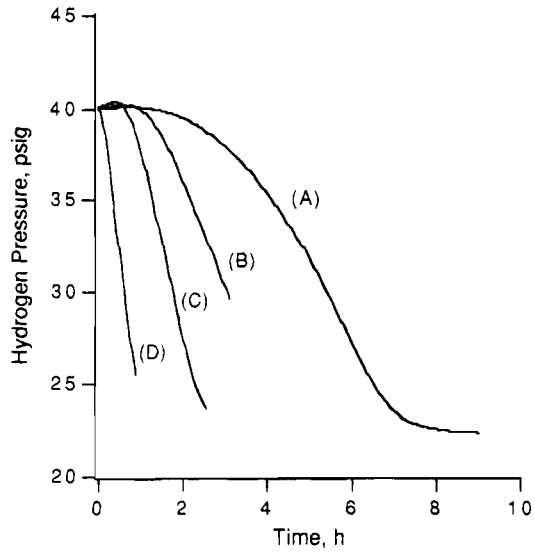

Figure 15. Effect of H_2O on cyclohexene hydrogenation beginning with the precatalyst **1**: (A) 80 equiv of H_2O (equiv vs starting 1.18 mM **1**; this is the background H_2O present in commercial Burdick & Jackson acetone); (B) with 1180 equiv of H_2O added; (C) with 1660 equiv of H_2O added; (D) with 5600 equiv of H_2O added. In (C) and (D) (but not in (A) or (B)), a precipitate of bulk Ir(0) metal is observed. Note also that the hydrogenation curves for solutions with up to 770 equiv of added water (not shown) are virtually identical to curve (A), except that the induction period decreases with increasing water.

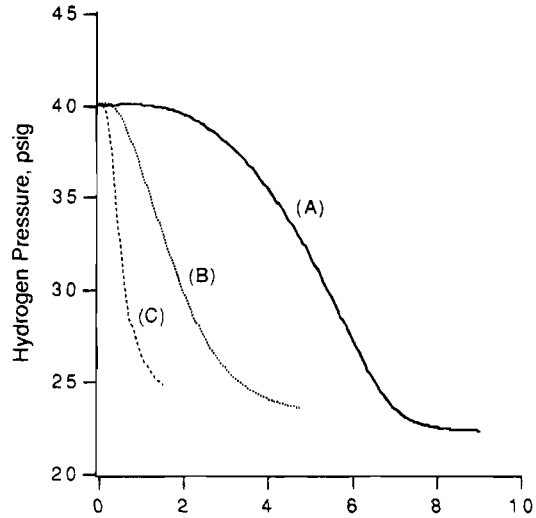

Figure 16. Effect of HOAc on cyclohexene hydrogenation beginning with **1**: (A) 0 equiv of HOAc; (B) 4.3 equiv of HOAc; (C) 61.0 equiv of HOAc (equiv vs the starting 1.2 mM **1**). A control with 90 equiv of $Bu_4N^+OAc^-$ showed no effect (i.e. showed a plot identical to curve (A)), indicating that the HOAc effect is a H^+ and not a OAc^- effect.

Also, HOAc was shown to greatly increase the $\{-d[H_2]/dt\}_{apparent}$ rate by 63% at 4.3 equiv and 580% at 61 equiv (vs the starting **1**), Figure 16, yielding a turnover number of ca. 6900 ± 2700, the highest TON measured in this work (recall Table 1).[47] A control reaction, in which 90 equiv of $Bu_4N^+OAc^-$ was added, shows no change whatsoever from a standard hydrogenation run, thereby demonstrating that the HOAc effect is due to H^+ and not OAc^-, Table 2. A TEM was taken of the precipitate from the experiment with 61 equiv of HOAc to see if the size or the distribution of the Ir nanoclusters had dramatically changed. The results and associated size-distribution histogram (Figure D, supplementary materials) show that neither the size (ca. 20 Å) nor the distribution of the Ir nanoclusters has changed significantly.

At least part of the decreased induction periods and faster *apparent* rates with H^+ or H_2O must be due to the expected cleavage of $Ir(1,5\text{-COD})(solvent)_2^+$ off of **1**, namely $(1,5\text{-COD})\text{-}IrP_2W_{15}Nb_3O_{62}^{8-} + H^+ (H_2O) + 2\ solvent \rightarrow Ir(1,5\text{-COD})(solvent)_2^+ + [H^+P_2W_{15}Nb_3O_{62}^{9-}]^{8-}$. Note that this reaction is an independent pathway that closely parallels, and achieves the same result as, the first reaction in Scheme 1 (eq 2) which leads to Ir nanocluster nucleation and growth. In addition, *a novel H^+-assisted hydrogenation catalysis mechanism is implied*, one that probably also operates on solid-oxide-supported $Ir_{\sim 190-450}$ heterogeneous catalysts. Hence, the details and intimate mechanism for this H^+-assisted catalysis are a high priority of our studies in progress.

(E) Brief Survey of Other Solvents. An in-depth survey of solvents was done very early on in our catalytic studies[7a,8a] (this was how Baker acetone distilled from K_2CO_3 was empirically selected for our early studies as it gives the fastest, soluble catalyst). Below, we briefly return to these solvent studies, primarily to show that the $Ir_{\sim 190-450}$ nanoclusters and their mechanism of formation, Scheme 2, can fully explain all of the observed data.

The reaction is highly solvent dependent, Table 2. In CH_3CN, the hydrogenation reaction proceeds without an induction period and a precipitate identified as bulk Ir(0) forms within 1 h. In dramatic contrast, in the more weakly coordinating solvent CH_2Cl_2, no cyclohexene hydrogenation is observed over even 38 h; similarly, in $C_2H_4Cl_2$ (1,2-dichloroethane), a very long induction, ca. 7 h period is observed followed by a rate 50% that normally seen in Burdick and Jackson acetone, Table 2. All of these solvent effect results can be understood in terms of dissociation of $Ir(1,5\text{-COD})(solvent)_2^+$, with increasing dissociation in more coordinating solvents like CH_3CN,[48] and then the rapid and independently verified[1] reduction of $Ir(1,5\text{-COD})(solvent)_2^+$ by H_2 to autocatalytically generate the active, $Ir_{\sim 190-450}$ nanoclusters (all as previously outlined in Scheme 1).[49]

(F) Attempted Catalyst Recovery Experiments Using CO or 1,5-COD. Heterogeneous catalysts composed of bulk Rh rafts can be essentially quantitatively converted to their supported $Rh(CO)_2$ analogs[50] (we are unaware of an analogous report for *iridium*, however). Hence, it was conceivable and

(47) A caveat here is that the *apparent* rate comparisons provided, $\{-d[H_2]/dt\}_{apparent}$ (see the Experimental Section), may not reflect the true relative rates. Additional studies with isolated $Ir_{\sim 190-450}$ nanoclusters, and measuring the true $\{-d[H_2]/dt\}_{initial}$, will be needed to fully understand these interesting H^+ and H_2O effects, and such studies are in progress. Even with the above caveat, however, the size of the HOAc-induced rate enhancement suggests a change in the *mechanism* of olefin hydrogenation on the $Ir_{\sim 190-450}$ nanoclusters.

(48) One other quite interesting point about the mechanism of formation of the nanoclusters is apparent from the CH_3CN data. The two key observations are that (i) authentic $Ir_{\sim 190-450}$polyoxoanion nanoclusters made and isolated from acetone *are stable in CH_3CN*, yet (ii) the use of CH_3CN leads to bulk Ir(0) (due to too much dissociation of **1** to $Ir(1,5\text{-COD})(CH_3CN)_2^+$, which in turn leads to an excessively rapid production of Ir(0) and thus a bulk Ir(0) precipitate). These observations provide excellent evidence in support of $Ir_{\sim 190-450}$ nanocluster formation as requiring the *slow, kinetically controlled* generation of Ir(0) atoms and their resultant *controlled nucleation* to Ir nanoclusters, all as previously deduced on the basis of other evidence[1] and as shown in Scheme 1.

(49) These solvent effect results stand in contrast, for example, to Crabtree's homogeneous hydrogenation catalyst,[19,32] $[Ir(1,5\text{-COD})(PPh_3)_2]PF_6$, in which the *less coordinating solvents* CH_2Cl_2 and 1,2-dichloroethane are the optimum solvents. These opposite solvent effects help emphasize the difference between the present polyanionic $Ir_{\sim 190-450}$polyoxoanion nanoclusters and Crabtree's homogeneous catalyst.

(50) Prins has reported that ultradispersed *rhodium* on alumina, which exists as small crystallites under hydrogen, disperses when exposed to 1 atm CO at room temperature to produce supported $Rh^I(CO)_2$: van't Blik, H. F. J.; van Zon, J. B. A. D.; Huizinga, T.; Vis, J. C.; Koningsberger, D. C.; Prins, R. *J. Am. Chem. Soc.* **1985**, *107*, 3139.

Scheme 2. Alkene and Polyoxoanion Reduction by $Ir_{\sim 190-450}$ Polyoxoanion Nanoclusters

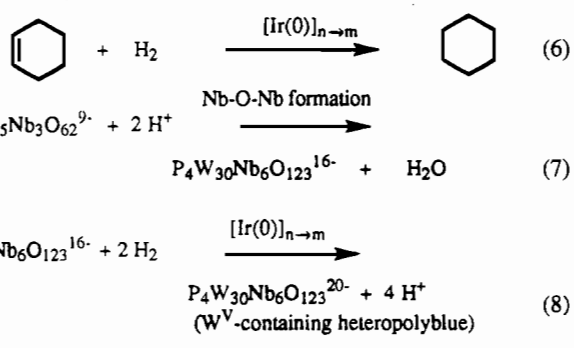

worth testing that the $Ir_{\sim 190-450}$ polyoxoanion nanoclusters could be broken up to form the known[51] $[(OC)_2Ir{\cdot}P_2W_{15}Nb_3O_{62}]^{8-}$ under CO pressure. When an amber acetone solution of $Ir_{\sim 190-450}$ nanoclusters (2 mg/mL) was subjected to 10 psig CO, *no detectable* formation of $[(OC)_2Ir{\cdot}P_2W_{15}Nb_3O_{62}]^{8-}$ occurred (by IR, in comparison to authentic material) and a TEM of CO-treated solution deposited on a carbon-coated Cu grid showed no observable change in the ca. 20 Å Ir nanoclusters.

Similarly, even 210 equiv of added 1,5-COD failed to give any recovery (i.e., conversion of the $Ir_{\sim 190-450}$ nanoclusters) to the precatalyst, **1**.

(4) Polyoxoanion/Bu_4N^+-Stablized $Ir_{\sim 190-450}$ Nanocluster Catalysts and Their Classification as "Hybrid Homogeneous–Heterogeneous Catalysts". All of the data presented herein, as well as the evidence provided earlier[1] for the nanocluster nucleation and growth mechanism presented in Scheme 1, can only be explained by the isolable $Ir_{\sim 190-450}$ nanoclusters, or their fragments which are also nanoclusters, being the true catalysts in the hydrogenation of cyclohexene (plus the reduction of the polyoxoanion to a heteropolyblue[1]) beginning with **1**, Scheme 2 (refer back to Scheme 1 if needed for the origin of the H^+ required in Scheme 2).

Note, however, that we have only a single piece of (non-definitive) evidence about which of the specific clusters within the distribution of $Ir_{\sim 190-450}$ or "$Ir_{\sim 300}$" nanoclusters are active (nor has this question ever been answered in the literature). The finding that the average TON for the $Ir_{\sim 190-450}$ nanoclusters presented in Table 1 assumed that all the surface Ir is active (i.e., 20–50% of all the initial Ir), and the fact that this calculation led to a TON (i.e., per Ir atom) consistent with independently measured TONs for authentic Ir(0) catalysts, suggests (as one might expect) *that all the different sized $Ir_{\sim 190-450}$ nanoclusters are active,* at least for structure-insensitive reactions such as hydrogenations.[52] However, nothing is known about the relative activity of these (or virtually any other) soluble metal nanocluster. This is especially true, we have realized, as one goes from a *structure ("cluster-size") insensitive* reaction, such as the present case of catalytic hydrogenation, to a *structure sensitive* reaction.[52] Probing metal(0) nanoclusters reactions as a function of nanocluster size, with both structure sensitive and insensitive reactions, is another of our future goals made possible by the identification of these *isolable* nanocluster catalyst materials.

Finally, it is useful to return for a moment to the "homogeneous or heterogeneous catalyst" classification presented earlier in Figure 2. By this classification scheme, the present $Ir_{\sim 190-450}$ nanoclusters are, strictly speaking, "heterogeneous-soluble" catalysts. However, the reproducible and narrow (homogeneous-like) size distribution of the $Ir_{\sim 190-450}$ nanoclusters, and their ±10% reproducible (and thus very homogeneous-like) reactivity, argues that the $Ir_{\sim 190-450}$ nanoclusters are better classified as a "hybrid heterogeneous–homogeneous catalyst".[53]

Summary

In summary, the following are the major findings of the present mechanistic studies: (1) A more general approach to the "homogeneous/heterogeneous" problem has been developed, an approach that emphasizes (i) early TEM studies, (ii) catalyst isolation studies, (iii) kinetic studies (especially quantitative explanation of any induction periods observed), (iv) quantitative phenomenological studies (with associated control experiments), and (v) the principle that the correct catalyst and mechanism will explain *all the data.* (2) The approach developed has been successfully applied to the cyclohexene hydrogenation catalyst derived from the polyoxoanion-supported Ir complex, $(Bu_4N)_5Na_3[(1,5\text{-COD})Ir{\cdot}P_2W_{15}Nb_3O_{62}]$, results which reveal that unprecedented, polyoxoanion/Bu_4N^+ $Ir_{\sim 190-450}$ nanoclusters are the true, "hybrid homogeneous/heterogeneous" catalysts. (3) The $Ir_{\sim 190-450}$ nanocluster catalysts can be reproducibly formed, exhibit an unprecedented ±10% reproducibility in their catalytic reactivity (at least toward the structure-insensitive reaction, cyclohexene hydrogenation), have been well characterized, and possess the important properties of being readily isolable and redissolvable. (4) The present polyoxoanion/Bu_4N^+ stabilized $Ir_{\sim 190-450}$ nanoclusters are the first examples of a soluble and reactive metal nanocluster in contact with, and (weakly) supported by, a soluble metal oxide. (5) The $Ir_{\sim 190-450}$ nanoclusters were found to have an Ir(0)-like reactivity with a TON as high as even the most highly dispersed and well-characterized Ir(0) catalyst available, Exxon's 80% dispersed 1% Ir on Al_2O_3; also of interest is the ca. 600% faster rate, and change in mechanism, for the hydrogenation reaction when HOAc was added, results which suggest a H^+-assisted hydrogenation mechanism that is under further investigation. (6) A variety of phenomenological studies were also examined (PPh_3 poisoning; Hg test; attempted CO recovery), results which should aid others in choice of the best homogeneous vs heterogeneous tests in other systems. (7) The interesting and previously unrecorded and unquantitated effects of added H_2O, added H^+, and different solvents were chronicled and were explained primarily in terms of how these variables influence the nanocluster nucleation and autocatalytic growth steps. (8) The present results, especially the time and effort the present studies required—*even when we were correctly focused from the start toward a metal "colloid"*[10]—plus our intuition from reading the literature, suggest that colloids and nanoclusters are probably much more widespread than is generally appreciated as the true catalysts in ostensibly "homogeneously" catalyzed *reductive* reactions (two examples worthy of further scrutiny were cited in Table A).[54] (9) And, last, several interesting areas worthy of further investigation were identified.[55]

The above findings confirm our impressions from reading the extensive and growing[56] colloid literature: despite the extensive prior literature, quantitative studies of especially monodispersed colloids or nanoclusters, as well as detailed

(51) See elsewhere for the syntheses and characterization of $[(OC)_2M{\cdot}P_2W_{15}Nb_3O_{62}]^{8-}$ (M = Ir[8a] and Rh[7a]) complexes.

(52) For a lead reference to structure sensitive vs insensitive reactions, plus a study of the relevant case of heterogeneous Rh(0) catalysis of cyclohexene hydrogenation, see: Boudart, M.; Sajkowski, D. J. *Faraday Discuss.* **1991**, *92*, 57, and references therein.

(53) Another issue here is whether or not the classification scheme as presently written is effectively reaction dependent (i.e., it appears that the classification scheme as now configured may be reaction dependent). Hence, Figure 2 may have to be modified eventually to restrict truly homogeneous (single type of active site) catalysts to those exhibiting true homogeneity in their active sites when scrutinized with the more rigorous probe of a structure sensitive[52] reaction.

mechanistic studies of colloid and nanocluster formation or of their subsequent reactions, are little explored but exciting subjects.

Experimental Section

Materials. $(Bu_4N)_5Na_3[(1,5\text{-COD})IrP_2W_{15}Nb_3O_{62}]$ (**1**),[6,8a] $(Bu_4N)_4Na_2[(1,5\text{-COD})IrSiW_9Nb_3O_{40}]$ (**2**),[38] and $[(1,5\text{-COD})IrCl]_2$[6,8a] were prepared according to the literature. All commercially obtained compounds were Baker reagent grade unless specified. Hydrogen gas (Air Products, 99%) was purified by passing through an indicating moisture trap, a disposable O_2 cartridge, and an indicating O_2 trap (Scott). *The source, purity, and pretreatment of the acetone solvent was discovered to be crucial for the reproducibility of the catalytic work described herein*; induction periods and rates differing by 300% are possible in wet vs dry but otherwise identical acetone solvent, for instance (see the text for further details). Acetone from Burdick & Jackson (containing 0.2% water) was used as received for all hydrogenation studies unless specified; Baker acetone (as received, containing 0.3% water, or distilled from K_2CO_3) was used only early on in the present studies or for comparison purposes (where indicated in the text). The H_2O content of the solvents used herein was determined by a recent literature method[44] employing a water-sensitive dye and UV−visible spectroscopy. [Note that, although purification texts[57] suggest K_2CO_3 as a way to *initially dry* acetone, longer contact with K_2CO_3 instead produces base-catalyzed aldol condensations plus water.[46]] Cyclohexene was purified and rendered peroxide free by passing it through a Brockman activity I basic alumina (Fischer) column and then distilling it from Na under N_2. The solvents CH_3CN, CH_2Cl_2, and $C_2H_4Cl_2$ (1,2-dichloroethane) were distilled from CaH_2 under N_2 and were then transferred immediately into the drybox where they were stored. $AgSbF_6$ (Aldrich), HOAc, and Hg (triply distilled, Quicksilver products) were used as received. PPh_3 (Aldrich) was recrystallized from methanol (mp 80.5−81 °C; lit.[58] mp 80−81 °C). Dr. G. B. McVicker of Exxon Research generously supplied a well-characterized[37] sample of 80%-dispersed 1% Ir on η-alumina; it was activated by reducing under a stream of H_2 (500−1000 cm^3/min H_2 flow rate) and at a temperature of 300−350 °C. A lower, 7.9%-dispersed 1% Ir/γ-Al_2O_3 was obtained commercially from Aesar; the sample was used as received and the hydrogen chemisorption data for this sample were obtained from Micromeritics, Norcross, GA. A sample of $(Bu_4N)_4Na_2[(1,5\text{-COD})IrSiW_9Nb_3O_{40}]$, **2**, used in several control or reference experiments, was prepared and its purity verified as described in detail elsewhere.[38]

Instrumentation and Analytical Procedures. All air-sensitive materials were routinely manipulated in a Vacuum Atmospheres N_2-filled inert-atmosphere drybox (containing ≤1 ppm O_2 as monitored by a Vacuum Atmospheres O_2 gauge). IR spectra were measured as KBr pellets on a Nicolet 5DX spectrometer. ^{1}H NMR spectra were recorded in 5 mm o.d. tubes on a General Electric QE-300 spectrometer at 20 °C, and the chemical shifts were reported using the δ scale referenced to the ^{1}H residual of the deuterated solvent. UV−visible spectra were recorded on a Beckman DU-7 spectrophotometer using 1-cm cells equipped with Teflon stoppers for all air-sensitive samples. Gas−liquid chromatography (GLC) was performed on a Hewlett Packard HP5970A GLC equipped with a HP 3390A integrator, an Alltech Econo-cap Capillary Carbowax column (30 m × 0.25 mm), and a flame ionization detector (FID). The following column temperature program was used in all GLC studies: initial temperature 35 °C for 4.0 min; ramped at 15 °C/min to a final temperature of 200 °C and held there for 1.0 min, followed by cooling back to 35 °C.

Transmission Electron Microscopy (TEM). Details for the TEM studies are provided elsewhere, including a variety of control experiments which showed the samples examined both are beam stable and are also representative of the bulk sample.[1]

Solution Molecular Weight Measurements. Weight-average solution molecular weights, $\bar{M}_r$, were determined by the ultracentrifuge sedimentation−equilibrium method.[59] Samples were prepared and loaded in the ultracentrifugation cell in the drybox, and the experiments were carried out on a Beckman Instruments Spinco Model E ultracentrifuge equipped with a scanning photoelectric system and an on-line IBM-compatible computer. All other experimental details (including controls for the air sensitivity of the ultracentrifugation cell, plus details of the data analysis) were exactly as described in an accompanying paper.[1]

Hydrogenations. The hydrogenation of cyclohexene was carried out in a 18 × 150 mm disposable borosilicate culture/tube placed in a Fisher-Porter bottle, which had been modified with Swagelok TFE-sealed quick-connects. The Fischer-Porter bottle was placed in a constant-temperature water bath regulated at 22.0 ± 0.1 °C via a Neslab Escal temperature-controlling bath and then connected between the pressure transducer and the H_2 pressure line via the quick-connects. Before connection, the pressure line and transducer were evacuated for more than 0.5 h and back-flushed with H_2 three times. The Fischer-Porter bottle was purged 15 times with H_2 (15 s per purge) and shaken vigorously for 30 s to allow for the equilibration between hydrogen gas and the liquid reaction mixture. Then, the hydrogen pressure was set at 40.0 ± 0.5 psig, the reaction was initiated by vortex stirring of the solution (a setting of at least 6 on a VWR Model 310 magnetic stirring plate), and the hydrogen pressure vs time data collection was started (t = 0 was set after the purging and vigorous shaking steps were completed).

Control experiments showed that the reaction is not stirring-rate-dependent at this stirrer setting,[60] a result confirmed by the observation of *chemical* (vs mass-transfer, diffusion-limited) kinetics under these conditions. The progress of the hydrogenation reaction was monitored (over periods ranging from 2−40 h) by the loss of the hydrogen pressure detected using a Omega PX621 pressure transducer interfaced through an Omega WB-35 "White Box" A/D converter to a IBM PC-XT using the RS-232 module of Lotus Measure. (A detailed drawing of the complete hydrogenation apparatus is shown in Figure 6.) The data were then fed into LOTUS 123 and worked up from there.

A control experiment, done by D. Lyon,[8a] using air-sensitive deep-blue $Co^I(CO)[(C_2)(DO)(DOH)_{pn}]$[61] (1 mM in acetone under 40 psig *argon*) showed that O_2 leakage into the Fischer-Porter bottle is insignificant over 15 h, as the color did not fade during this time period (the blue turns to yellow in less than 3 s if the solution is deliberately exposed to air). This control experiment was performed under argon instead of hydrogen, since there is a reaction between the deep blue

(54) (a) Conversely, many ostensibly heterogeneous-insoluble catalysts may actually involve homogeneous-soluble catalysis by discrete complexes or clusters leached off the support surface, a related but little studied mechanistic issue of "heterogeneous" catalysis. (b) Parshall, G. W.; Ittel, S. D.; *Homogeneous Catalysis*, 2nd ed.; John Wiley, Inc.: New York, 1992 (see p 110, 2nd paragraph, and p 118, also the 2nd paragraph). (c) Crabtree, R. H. *CHEMTECH* **1982**, 506. (d) Jones, R. A.; Seeberger, M. H. *J. Chem. Soc., Chem. Commun.* **1985**, 373.

(55) The polyoxoanion-dispersed and -stabilized $Ir_{\sim 190-450}$ nanoclusters may also be of interest for solid-state reactions and for further comparisons to conventional oxide-supported Ir(0) catalysts.

(56) (a) Esumi, K.; Tano, T.; Meguro, K. *Langmuir* **1989**, *5*, 268. (b) Lewis, L. N.; Lewis, N. *Chem. Mater.* **1989**, *1*, 106−14. (c) Satoh, N.; Kimura, K. *Bull. Chem. Soc. Jpn.* **1989**, *62*, 1758−63. (d) Bradely, J. S.; Hill, E. W.; Klein, C.; Chaudret, B.; Duteil, A. *Chem. Mater.* **1993**, *5*, 254. (e) Deteil, A.; Queau, R.; Chaudret, B. *Chem. Mater.* **1993**, *5*, 341. (f) Schueller, O. J. A.; Pocard, N. L.; Huston, M. E.; Spontak, R. J.; Neenan, T. X.; Callstrom, M. R. *Chem. Mater.* **1993**, *5*, 11. (g) Andrews, M. P.; Ozin, G. A. *Chem. Mater.* **1989**, *1*, 174 and the references herein. (h) Klabunde, K. J.; Habdas, J.; Cárdenas-Triviño, G. *Chem. Mater.* **1989**, *1*, 481. (i) Zuckerman, E. B.; Klabunde, K. J.; Olivier, B. J.; Sorensen, C. M. *Chem. Mater.* **1989**, *1*, 12−14. (j) Lin, S.-T.; Franklin, M. T.; Klabunde, K. J. *Langmuir* **1986**, *2*, 259. (k) Cárdenas-Triviño, G.; Klabunde, K. J.; Dale, E. B. *Langmuir* **1987**, *3*, 986−92. (l) Bradley, J. S.; Hill, E.; Leonowicz, M. E.; Witzke, H. *J. Mol. Catal.* **1987**, *41*, 59−74.

(57) Base-catalyzed aldol reactions of acetone are presumably why Perrin and Perrin's text (see p 24)[58] recommends that "... K_2CO_3 ... is suitable for an *initial drying* of alcohols, bases, esters, ketones and nitriles by *shaking with them and then filtering off* the K_2CO_3".

(58) Perrin, D. D.; Armarego, W. L. F.; Perrin, D. R. *Purification of Laboratory Chemicals*, 2nd ed.; Pergamon: Oxford, U.K., 1980; p 455.

(59) (a) Chervenka, C. H. *A Manual of Methods for the Analytical Ultracentrifuge*; Spinco Division of Beckman Instruments: Palto Alto, CA. (b) Fujita, H. *Foundations of Ultracentrifugal Analysis*; John Wiley & Sons, Inc: New York, 1975; pp 308−313. (c) Droege, M. W. Ph.D. Thesis, University of Oregon, 1984.

(60) See pp 106−107 in the Ph.D. thesis of D. Edlund.[7a]

(61) Finke, R. G.; Smith, B. L.; McKenna, W. A.; Christian, P. A. *Inorg. Chem.* **1981**, *20*, 687.

Co(I) complex and hydrogen which causes the solution to turn deep brown over ca. 5 h.

Additional control experiments, done by D. Lyon,[8a] demonstrate the accuracy of the data collected with the Omega PX621 transducer and digitized with the Omega A/D converter. This control experiment, cyclohexene hydrogenation catalyzed by $[Ir(1,5\text{-COD})(PPh_3)_2]PF_6$ [32] in 1,2-dichloroethane, involved demonstrating that the initial turnover frequencies (in mmol of H_2·mmol of precatalyst^{-1}·h^{-1}) are within experimental error for data collected by reading a 0−60 psig pressure gauge (calibrated in ±0.2 psig increments) and for data (in an independent but otherwise identical experiment) collected using the pressure transducer and the A/D converter. These results were the same within experimental error: $TOF_{initial}$(pressure gauge) 530 ± 80 h^{-1}; $TOF_{initial}$(digitized) 625 ± 100 h^{-1}. Further control experiments showed that the hydrogenation apparatus experienced less than 1 psig pressure loss over 15−20 h (most experiments were monitored less than 10 h) compared to the 18 psig of H_2 pressure loss due to a Standard Conditions cyclohexene hydrogenation over ca. 8 h. (Small amounts of hydrogen pressure leakage, about 5−7 psig over 40 h, were observed in some longer experiments. In such longer experiments, where only the total turnover number (TON) is of interest, the TON was calculated from the ^{1}H NMR analysis described next.)

In a fourth type of control, the cyclohexene conversion was checked by NMR and compared to the amount expected from the H_2 uptake, to be sure that they agreed to within ± 5%. This was done by determining the ^{1}H NMR integral of the cyclohexene peak (δ 5.41 (CH), in $CDCl_3$) and the cyclohexane peak (δ 1.17 (CH_2), in $CDCl_3$). In this analysis, the addition of $CDCl_3$ to the catalyst solution caused the polyoxometalate to precipitate as a fluffy white solid, which conveniently removed the interfering Bu_4N^+ cation resonances. GLC was used to confirm that the precision of the ^{1}H NMR integrals is ±5%.

The following precautions were taken to avoid the possibility of catalytic activity due to contamination of the reaction culture tubes or the magnetic stir bars with either Ir(0) or the precipitated catalyst: the culture tubes were disposed of after each experiment, and the magnetic stirring bars were washed with acetonitrile and rinsed with acetone, followed by a careful visual examination. If the stir bars appeared to be contaminated, they were simply discarded. Only clean stir bars (without any particles or coated films) were reused. Control experiments show that the above precautions yielded stir bars free from Ir(0) or other catalyst(s) as judged by their inability to catalyze cyclohexene hydrogenation.

The *apparent turnover rate*, $\{-d[H_2]/dt\}_{apparent}$ in mmol of H_2/h, for cyclohexene hydrogenation in a given experiment was obtained from the ±10% reproducible slope of the linear part of the hydrogen uptake vs time curve and then converted into the proper units (mmol of H_2/h) using the idea gas law, $PV = nRT$, and the measured total volume of the system, V = 97 mL (determined volumetrically using H_2O). Note that the cyclooctane evolution curve (Figure 7, inset) demonstrates that it takes ca. 8 h for all the $(Bu_4N)_5Na_3[(1,5\text{-COD})IrP_2W_{15}Nb_3O_{62}]$, **1**, precatalyst to evolve into catalyst. This fact, and the autocatalysis observed after the ca. 2 h induction period, mean that the apparent turnover numbers obtained in this fashion are not true turnover numbers [i.e., they cannot be, as the catalyst is still forming and should make the reaction go (autocatalytically) faster and faster; the linear part is apparently a fortuitous balance between this opposite and expected slowing of the reaction as it runs out of cyclohexene and H_2 (assuming nonzero order cyclohexene or H_2 rate dependencies as preliminary numerical-integration kinetic studies suggest[8a])]. However, the reproducible $\{-d[H_2]/dt\}_{apparent}$ (typically 1.1 ± 0.1 mmol of H_2/h) proved adequate for most of the present studies where only relative apparent rates were needed. Where estimates of the true *initial* rates for H_2 uptake, $\{-d[H_2]/dt\}_{initial}$, were needed, these were obtained from the $\{-d[H_2]/dt\}_{initial}$ part of the P_{H_2} vs time plot *using isolated nanocluster catalyst* and were then converted into the proper mmol of H_2/hr units using the ideal gas law.

Initial turnover numbers, $TON_{initial}$, were calculated for the isolated catalysts from the $\{-d[H_2]/dt\}_{initial}$, and using the experimental fact that 0.2 equiv of PPh_3 totally poisons a completely active catalyst (i.e., calculated by assuming that 20% of the Ir atoms present are catalytically active); hence, the $\{-d[H_2]/dt\}_{initial}$ = 1.7 mmol H_2/h for isolated catalyst (see the sections which follow; see also Table 1) corresponds to a $TON_{initial} \approx$ 2430/h [i.e., (1.7 mmol/h)/(0.2 × 0.0035 mmol of precatalyst **1**)]. Alternatively, as a check, a $TON_{initial} \approx$ 970/h is obtained (i.e., 1.7 mmol/h)/(0.5 × 0.0035 mmol of precatalyst **1** from approximating the $Ir_{\sim 300}$ average nanoclusters as cubic-closed-packed spheres and from the estimate that roughly 50% of the $Ir_{\sim 300}$ atoms should be on the surface[36] plus the assumption that all surface Ir are active. Similarly, using the inset in Figure 7 to estimate that only ca. 40% of the precatalyst **1** typically evolves into nanoclusters when the reproducible $\{-d[H_2]/dt\}_{apparent}$ = 1.1 ± 0.1 mmol of H_2/h is measured, and using the 0.2 equiv of PPh_3 result above, yield a $TON_{apparent} \approx$ 3930/h for nonisolated catalyst (i.e., 1.1 mmol/h)/(0.2 × 0.4 × 0.0035 mmol of precatalyst **1**). The value of 3200 ± 1000 reported in Table 1 for **1** is an average of the 3930 and 2430 TONs.

Standard Conditions for Cyclohexene Hydrogenation Starting with the Precatalyst 1. In the drybox, 20.0 ± 2.0 mg ((3.53 ± 0.35) × 10^{-3} mmol) of $(Bu_4N)_5Na_3[(1,5\text{-COD})IrP_2W_{15}Nb_3O_{62}]$, **1**, was dissolved in 2.5 mL of Burdick & Jackson degassed acetone, followed by the addition of 0.5 mL (4.94 mmol) of purified cyclohexene. The clear bright-yellow solution (containing 1.2 ± 0.1 mM of **1** and 1.65 M of cyclohexene) was then transferred to an 18 × 150 mm disposable borosilicate culture tube which contained a 0.5 in. stir bar. The tube was placed in a Fischer-Porter bottle, the bottle was sealed and brought out of the drybox, the Fischer-Porter bottle was attached via the quick-connects (and using the evacuation, H_2 flush procedure indicated under "Hydrogenations" above), and the reaction was started with an initial 40 psig of hydrogen pressure, vigorous shaking, and vortex stirring, all as detailed under "Hydrogenations" above.

After a reproducible 2.0 ± 0.2 h induction period (i.e., reproducible so long as the source of the acetone solvent, its H_2O content, and the other variables are the same), an easily detected ≥0.05 psig H_2 pressure loss was observed *that was used to define the end of the induction period.* After this induction period, an autocatalytic burst of catalytic activity is seen, followed by a roughly linear H_2 consumption rate of $\{-d[H_2]/dt\}_{apparent}$ = 1.1 ± 0.1 mmol of H_2/h. As the reaction proceeds, the original clear-yellow solution gradually turns turbid yellow-brown and then an intense blue indicative of the formation of a reduced, W^V-containing "heteropolyblue"[62] polyoxoanion once the cyclohexene hydrogenation reaction is ca. 90% complete. The blue color is lost immediately if the reaction solution is exposed to air or if the H_2 pressure is released (the blue color fades within ca. 30 min after the H_2 pressure is released even if the Fischer-Porter reaction vessel is taken into the drybox). The blue color is not essential to catalysis (for example, the isolated catalyst loses its blue color but retains its catalytic activity).

It is noteworthy that the above hydrogenation reaction *has been repeated more than a hundred times, by two different researchers,*[8a] and that the hydrogenation rate and other results are reproducible within 10% *provided* one uses *the same source of acetone* and if the concentrations and other variables are kept constant.

Generation of the Cyclooctane Evolved vs Time Curve during Cyclohexene Hydrogenation Beginning with the Precatalyst, 1. Using a bright-yellow solution of 1.2 ± 0.1 mM of **1** and 1.65 M of cyclohexene in Burdick & Jackson acetone containing 0.5 μL of toluene (as a GLC internal standard), the cyclohexene hydrogenation reaction was started with an initial H_2 pressure of 40.0 psig as described above (see the "Standard Conditions" section). Five total, independent reaction runs were performed; each run was stopped by releasing the H_2 pressure at five predetermined times (after 1.7, 3.2, 4.6, 5.9, and 9.0 h of hydrogenation), and an aliquot was taken for GLC analysis with toluene as the internal standard. In addition, an absolute calibration curve of GLC peak area vs concentration of cyclooctane was obtained and was also used to determine independently the cyclooctane produced from **1** during the hydrogenation reaction. The results from the toluene internal standard and the absolute calibration curve methods both agreed within 15%. The production of cyclooctane vs time, summarized in the inset in Figure 7, is as follows: 0.02 equiv, 1.7 h; 0.09 equiv, 3.2 h; 0.3 equiv, 4.6 h; 0.5 equiv, 5.9 h; 1.0 equiv, 9.0 h (i.e., the final yield of cyclooctane is 1.0 ± 0.2). [Small amounts (<0.2 equiv) of cyclooctene (i.e., half-reduced cyclooctane) were also observed after

(62) Lead references include: (a) ref 2a, pp 101−117, and the references there in. (b) Pope, M. T. In *Mixed-Valence Compounds*; Brown, D. B., Ed.; Reidel: Dordrecht, The Netherlands, 1980; p 365. (C) Buckley, R. L.; Clark, R. J. H. *Coord. Chem. Rev.* **1985**, *65*, 167.

ca. 1.7 h, but this intermediate decreased with additional time to a final yield of 1.0 equiv of cyclooctane.]

Isolation and Characterization of the $Ir_{\sim 190-450}$ Nanoclusters Derived From Precatalyst 1. Cyclohexene hydrogenation was carried out exactly as described in the "Standard Conditions" section detailed above. After 9 h, when all the 20 mg of precatalyst **1** had been converted to the active catalyst (Figure 7, cyclooctane evolution inset), the reaction was effectively terminated by simply stopping the vortex stirring (thereby preventing efficient H_2 gas-to-solution mixing). The Fischer-Porter bottle was then disconnected from the H_2 line via the quick-connects and brought back into the drybox. The 40 psig H_2 pressure was released, and the $Ir_{\sim 190-450}$ polyoxoanion product (as partially characterized elsewhere[1] and as further identified below) was isolated as a brown precipitate, by filtering through a Whatman No 2 paper, or as a dark-brown powder, by gravity sedimentation in a centrifuge tube following removal of the light-yellow-brown supernatant and drying under vacuum overnight at ambient temperature. A total of 6.0 mg of dark-brown powdered $Ir_{\sim 190-450}$ polyoxoanion was isolated from the product solutions of two hydrogenation runs (i.e., 3.0 mg of $Ir_{\sim 190-450}$ polyoxoanion was obtained from each of two single hydrogenation runs starting with 20 mg of precatalyst **1**). Elemental analysis of the $Ir_{\sim 190-450}$ polyoxoanion sample containing ca. 12 mg isolated from four hydrogenation runs (Pascher, Germany, handling under N_2) is as follows. Found: C, 14.03; H, 2.57; N, 0.99; P, 0.76; Ir, 14.2; O, 15.5. Calc for $[Ir_9(P_4W_{30}Nb_6O_{123})(Bu_4N)_9Na_7]_{\sim 33}$: C, 14.13; H, 2.67; N, 1.03; P, 1.01; Ir, 14.14; O, 16.08.

The $Ir_{\sim 190-450}$ nanoclusters are soluble in acetone and are more soluble in acetonitrile, giving an amber solution that is "homogeneous" to the naked eye. [Note that this solubility alone rules out the presence of bulk (and thus insoluble) Ir(0) metal particles in either the brown precipitate or the hydrogenation runs starting with precatalyst **1**.]

TEM of the amber solution (ca. 0.5 mg of $Ir_{\sim 190-450}$ polyoxoanion/mL of CH_3CN, sprayed onto a copper grid covered with an amorphous carbon thin film) showed the presence of dark, almost spherical ca. 20 Å particles surrounded by small granular particles, Figure 8. The 20 Å particles were unequivocally identified to be Ir(0) nanoclusters by electron diffraction studies, as detailed elsewhere.[1] The small, granular particles proved to be polyoxoanion as visualized separately (following spraying of a ca. 0.5 mM acetone solution of $(Bu_4N)_9P_2W_{15}Nb_3O_{62}$ or $(Bu_4N)_{12}H_4P_4W_{30}Nb_6O_{123}$ onto a carbon-coated Cu grid) in a TEM control experiment, presented in the accompanying paper.[1] Another TEM control experiment was conducted using precatalyst **1** (ca. 0.5 mM in acetone); the TEM image (presented elsewhere[1]) was indistinguishable from that of $(Bu_4N)_9P_2W_{15}Nb_3O_{62}$ (specifically, no dark, spherical particles of any sort were observed) demonstrating that the $Ir_{\sim 300}$ nanoclusters are not generated from any unreacted **1** under the TEM electron beam. Additional controls were also done (for example to ensure that the electron micrographs shown are representative of the bulk sample; for details, see "Transmission Electron Microscopy", in the Experimental Section, provided in an accompanying paper[1]).

The average size of the Ir nanoclusters, 20 ± 3 Å, was determined by counting 366 Ir nanoclusters; the resulting frequency vs nanocluster diameter histogram is shown in Figure 8. As detailed earlier (see[1] footnote 29), the 20 ± 3 Å Ir nanoclusters roughly correspond to $Ir_{\sim 190-450}$, with the average 20 Å size corresponding *approximately* to $Ir_{\sim 300}$.

The $Ir_{\sim 190-450}$ nanoclusters were also characterized by an ultracentrifugation molecular weight measurement, results that have already been described.[1] The result, $\bar{M}_r$ of 86 000 ± 40 000 (Figure A, supplementary material) is somewhat larger than the calculated MW range for $Ir_{\sim 190-450}$ of 36 480−86 400; this is due, presumably, to the presence of the polyoxoanion (see the discussion of this result in the text).

In two separate control experiments, the amber solution in both acetone (the solvent used for catalysis) and in CH_3CN (in which the Ir nanoclusters are more soluble) *but without added electrolyte* was spun at 20 000 rpm (a speed appropriate for a MW measurement of the polyoxoanion). Ten minutes later, the absorption in the 400−460 nm range characteristic of the Ir nanoclusters was reduced to zero, indicating that all Ir nanoclusters had deposited in the bottom of the ultracentrifuge cell. Indeed, careful visual checking of the ultracentrifuged solution (i.e., after the ultracentrifugation was finished) confirmed that the Ir nanoclusters had been deposited as a dark brown precipitate, leaving a clear, colorless supernatant (containing only polyoxoanions). However, the dark deposit of $Ir_{\sim 190-450}$ nanoclusters redissolved to re-form a clear, amber solution when the cell was shaken.

In a separate ultracentrifugation experiment, the MW of the polyoxoanions present along with the $Ir_{\sim 190-450}$ nanoclusters in the isolated precipitate was measured. An amber solution of the isolated catalyst material in CH_3CN was prepared in the drybox by dissolving ca. 3 mg of the isolated, brown catalyst precipitate in 2 mL of 0.1 M $Bu_4N^+PF_6^-$ in CH_3CN and further diluting it (ca. 10 times) until the adsorption at 280 nm is between 0.3 and 0.5. Under a rotation speed appropriate for detection of the polyoxoanions, 20 000 rpm, equilibrium was established after 17 h. The computed MW (see elsewhere for the appropriate equation[1]) is MW = 10 800 ± 2000, based on the slope of the linear plot of ln (adsorption) vs r^2 (Figure B, supplementary material) and a measured[7a] partial specific volume of 0.37 cm^3/g. This MW corresponds to the Nb−O−Nb-bridged aggregate, $P_4W_{30}Nb_6O_{123}^{16-}$, calculated FW = 8165.

An IR spectrum (in acetone solvent using septa-capped NaCl cells) was also obtained of the amber solution; bands characteristic of the $P_2W_{15}Nb_3O_{62}^{9-}$ polyoxoanion (and/or its Nb−O−Nb bridged aggregate, $P_4W_{30}Nb_6O_{123}^{16-}$) were observed at 951 and 800 cm^{-1} (other polyoxoanions bands were obscured by the solvent). No bands were detected between 2800 and 2000 cm^{-1}; thus a previous report of an Ir−hydride peak at 2255 cm^{-1} by D. Lyon[8a] appears to be in error. [The absence of the Ir−hydride IR peak is, however, consistent with D. Lyon's report (see pp 123−124 in his Ph.D. thesis[8a]) that no Ir−hydride peak is detectable in the reaction solution by ^1H NMR at either 20 or −40 °C, even after 3 h of data collection.]

Quantitative Kinetic Testing of the Isolated $Ir_{\sim 190-450}$ Nanoclusters. Evidence That the Nanoclusters Are the True Catalyst in the Hydrogenation of Cyclohexene Beginning with the Precatalyst 1. (1) Kinetic Testing of the $Ir_{\sim 190-450}$ Polyoxoanion Brown Precipitate Derived from 1. In an 18 × 150 mm disposable borosilicate culture tube containing a 0.5 in. magnetic stir bar, 3.0 ± 0.2 mg (i.e. 15% by weight of the initial 20 ± 0.1 mg of **1** used) of the $Ir_{\sim 300}$ polyoxoanion brown precipitate was dissolved in 2.5 mL of Burdick & Jackson acetone to give an clear, amber solution, and 0.5 mL of cyclohexene was added last, turning the solution slightly turbid. A cyclohexene hydrogenation experiment was then carried following the Standard Conditions and procedures described earlier. No induction period is observed, and the observed initial rate is $\{-d[H_2]/dt\}_{initial}$ = 0.77 ± 0.1 mmol of H_2/h (Figure 10). Note that this rate accounts for 70% of the typical 1.1 ± 0.1 mmol/h apparent rate (i.e., the roughly linear part after the induction period in Figure 9), yet only 15% by weight of $Ir_{\sim 190-450}$ polyoxoanion nanoclusters (vs the initial weight of precatalyst **1**) was used. This experiment also indicates that the induction period starting with precatalyst **1** is due to the time required for the formation of Ir nanoclusters.

(2) Demonstration That the Formation of Ir Nanoclusters Can Quantitatively Account for the Induction Period, and Autocatalysis, Seen in the Standard Hydrogenation Reaction Beginning with $(Bu_4N)_5Na_3[(1,5\text{-}COD)Ir\text{-}P_2W_{15}Nb_3O_{62}]$, 1. (a) Shortening of the Induction Period by the Addition of Isolated $Ir_{\sim 190-450}$ Nanocluster Catalyst or Added $Ir(1,5\text{-}COD)(acetone)_2^+$. $Ir_{\sim 190-450}$ nanoclusters, which were generated from 20.0 mg of precatalyst **1** under the standard hydrogenation conditions as described previously, were isolated by evacuation to dryness (10 h, at ambient temperature). They were then redissolved in the drybox in 3.0 mL of acetone to give a clear, amber solution of $Ir_{\sim 190-450}$ nanoclusters. Meanwhile, an acetone solution of precatalyst **1** (1.2 mM) was prepared in an 18 × 150 mm culture tube, to which 0.15 mL (1.7×10^{-4} equiv vs **1**) of the $Ir_{\sim 190-450}$ nanocluster solution was added, followed by the addition of 0.5 mL of cyclohexene. The culture tube was then placed in a Fischer-Porter bottle, the bottle was removed from the drybox and connected to the hydrogen line, and the hydrogenation experiments were carried out under the Standard Conditions. Significant shortening of the induction period was found (1.0 h vs the normal 2.0 h), and the hydrogenation reached the same final rate (i.e., $\{-d[H_2]/dt\}_{apparent}$ = 1.1 mmol of H_2/h) as found in a typical run starting with precatalyst **1** only. [The previously yellow solution also turned green within 0.5 h after the reaction was started (i.e., green due to the yellow solution plus the heteropolyblue that is formed).] In a second experiment, 8.3×10^{-4} equiv of $Ir_{\sim 190-450}$ nanoclusters was added to the reaction solution (containing 1.2 mM of

1 and 1.65 M of cyclohexene in acetone). This time, an even shorter induction period of 0.8 h was observed, with the same rate (i.e., $\{-d[H_2]/dt\}_{apparent} = 1.1$ mmol of H_2/h) as found in a typical run starting with precatalyst **1** only. (Again, the previously yellow reaction solution turned blue within 0.5 h after the reaction was started.) These results are plotted in Figure 10.

The experiments with added $Ir(1,5\text{-COD})(acetone)_2^+$ are described elsewhere;[1] the results are also provided in Figure 10.

(b) Quantitative GEAR/GIT Curve-Fitting of the H_2 Pressure Loss Curve Demonstrating That Only Autocatalysis Accounts for the Observed Induction Period. These numerical integration curve-fitting studies, presented originally in an earlier communication,[10a] are also discussed and the appropriate figures presented elsewhere.[1]

(c) Rates for Authentic Ir(0) Catalysts for Comparison Purposes. These early experiments with the Ir metal particle catalysts were performed, and the data were collected, by D. Edlund.[7a] Cyclohexene hydrogenation reactions were carried out in an 18 × 150 mm borosilicate culture tube placed in the Fischer-Porter bottle under the normal reaction conditions (except that the acetone was predried from 3 Å molecular sieves): 40 psig initial H_2 pressure, an initial cyclohexene concentration of 1.65 M, 22 °C, and vortex stirring so that the hydrogenation rate has become stirring-rate independent.[7a] The only other difference from a Standard Conditions hydrogenation, in addition to the use of acetone predried over 3 Å molecular sieve mentioned above, was the use of 0.5 mM authentic Ir(0) catalysts, 80% dispersed 1% Ir/η-Al_2O_3 (28.8 mg; supplied and characterized by Drs. R. G. McVicker and R. L. Garten at Exxon Research[37]), 7.9% dispersed 1% Ir/γ-Al_2O_3, or bulk Ir metal particles $[Ir(0)_n]$ (prepared from 75 mM $[(1,5\text{-COD})Ir(CH_3CN)_2]BF_4$ in acetonitrile plus H_2).[7a] (It is noted that after 10 years of storage under air, both these catalysts were deactivated, presumably due to oxidation, and gave very low or no activity for cyclohexene hydrogenation. Thus samples freshly reduced with H_2 need to be used.) The number of active iridium sites in the bulk $[Ir(0)_n]$ was obtained by preparing the large amount of sample (~0.25 g) required for a BET surface area measurement by reducing 0.31 g of $[(1,5\text{-COD})Ir(CH_3CN)_2]BF_4$ with hydrogen. This sample gave a BET surface area of 2.57 m^2/g; the BET data was obtained from Micromeritics, Norcross, GA. The number of surface iridium atoms/g was then calculated by assuming an atomic radius of 1.36 Å for each Ir(0) atom so that each Ir is assumed to have a surface area of 5.81×10^{-20} m^2 (this value is simply the area of a circle of radius = 1.36 Å) and that the Ir(0) atoms lie edge-to-edge. The turnover numbers (TONs) for bulk Ir(0), corrected for the number of surface Ir(0) atoms in this fashion, are summarized in Table 1 (along with uncorrected TONs as well, which show the ca. ±100% surface area variation of Ir(0) precipitates prepared in such fashion).

(d) Test of the (Lack of) Influence of Different Polyoxoanions. Cyclohexene Hydrogenation and Its Rate Starting with $(Bu_4N)_4Na_2[(1,5\text{-COD})Ir\text{-}SiW_9Nb_3O_{40}]$, 2. In an experiment that was otherwise identical to the cyclohexene hydrogenation Standard Conditions (and in "dry" Burdick and Jackson acetone), in the drybox 12.0 ± 1.0 mg of **2** (3.1×10^{-3} mmol, 1.0 mM) was placed in a Fischer-Porter bottle and dissolved in 2.5 mL Burdick & Jackson acetone followed by the addition of 0.5 mL of purified cyclohexene (4.94 mmol, 1.65 M) to give a clear yellow solution. The Fischer-Porter bottle was removed from the drybox and attached to the hydrogenation apparatus, and a standard cyclohexene hydrogenation (i.e., only using **2**, instead of **1**) was initiated in the usual fashion at 40 psig H_2 by vigorous shaking and vortex stirring. As the reaction proceeded, the originally clear-yellow solution of **2** turned turbid yellow-brown, virtually identical to the color changes observed for **1**. [No blue color was observed, however, presumably due to the more negative ca. −1.6 V vs SCE reduction potential of the $SiW_9Nb_3O_{40}^{7-}$ polyoxoanion or −0.6 V vs SCE reduction potential of its three Nb—O—Nb bridged aggregate, $Si_2W_{18}Nb_6O_{77}^{8-}$.][63] Significantly, and after a slightly longer induction period of 2.5 ± 0.3 h, the rate of H_2 loss (1.1 ± 0.1 mmol/h) for **2** is *identical* to that for **1**, entry 1 of Table 2, and Figure 11.

(3) Quantitative Phenomenological "Homogeneous" vs "Heterogeneous" Catalyst Tests. (a) Three Cycles of Cyclohexene Hydrogenation, Evaporation of the Catalyst-Containing Solution to Dryness, and Then Redissolving of the Catalyst and Its Reuse in a New Cycle of Cyclohexene Hydrogenation. The Standard Conditions were employed in a cyclohexene hydrogenation experiment beginning with 20.0 mg of **1** in Burdick and Jackson acetone; a typical ca. 2 h induction period was followed by autocatalysis, and a roughly linear H_2 uptake was observed, $-d[H_2]/dt_{apparent} = 1.0$ mmol of H_2/h. The hydrogenation reaction was stopped by halting the vortex stirring after 90% of the cyclohexene hydrogenation (i.e., 90% of the theoretical H_2 uptake) was completed. The product solution was then evacuated to dryness over ca. 5 h at ambient temperature (i.e., through the Fischer-Porter bottle ball-valve as shown in Figure 6), and the Fischer-Porter bottle was removed from the hydrogenation apparatus via the quick-connects and taken into the drybox. While still in the drybox, a second hydrogenation run was set up by recharging the Fischer-Porter bottle and its catalyst-containing solid with Burdick and Jackson acetone plus purified 1.65 M cyclohexene; a cloudy amber solution again resulted. Significantly, this second cyclohexene hydrogenation proceeded *without an induction period*, and the initial rate was $\{-d[H_2]/dt\}_{initial} = 1.7$ mmol of H_2 /h, which is 1.7 times faster than the $\{-d[H_2]/dt\}_{apparent} = 1.0$ mmol of H_2/h (the rate decreased as the H_2 and olefin were consumed; however, the data were not worked up further due to the complication of precipitation of the Ir nanocluster catalysts which occurs as cyclohexene is hydrogenated to the nonpolar cyclohexane, causing a precipitation of the ionic $Ir_{\sim 190-450}$polyoxoanion/Bu_4N^+ catalyst). The higher *initial* rate observed in this second run is as expected, since the catalyst is nearly completely formed and thus at higher concentration than anytime during a hydrogenation experiment starting with the precatalyst, **1**.

This second hydrogenation run was stopped by halting the vortex stirring, but this time after 70% of the cyclohexene had been hydrogenated (stopping this experiment at 70% or less reaction does not introduce complications, since all of the precatalyst **1** has long since evolved into the active catalyst). Again, the solution was evacuated to dryness under a vacuum at ambient temperature over 5 h, the Fischer-Porter bottle was taken back into the drybox, and a third and final hydrogenation experiment was initiated in this same Fischer-Porter bottle by recharging it with fresh acetone and 1.65 M cyclohexene (a cloudy amber solution again resulted) and then removing the Fischer-Porter bottle from the drybox and attaching it to the hydrogenation line and again pressurizing it with 40 psig H_2. The initial rate of this third run was $-d[H_2]/dt_{initial} = 1.0$ mmol of H_2/h, somewhat slower than the second run (presumably due to agglomeration of the Ir nanocluster and thus decreased surface area and active sites, although this has not yet been verified by TEM; the agglomeration reaction and its kinetics are under further investigation). The results of these three experiments are compared graphically in Figure 12.

(b) Quantitative Poisoning Test Using 0.2 equiv of Added PPh_3. In the drybox, 19.0 mg (3.35×10^{-3} mmol) of **1** was dissolved in 2.5 mL of acetone in a borosilicate culture tube containing a 0.5 in. magnetic stir bar, followed by the addition of 0.5 mL of fresh cyclohexene. The culture tube was placed inside a Fischer-Porter bottle, which was then sealed, removed from the drybox, and attached to the hydrogenation apparatus. The cyclohexene hydrogenation reaction was then initiated with 40 psig H_2 and vigorous shaking and stirring according to the Standard Conditions detailed earlier. The reaction was stopped 9 h later, when all the cyclohexene had been converted to cyclohexane (as judged from the now flat hydrogen pressure-loss curve) and when all the precatalyst **1** had evolved into the catalyst (recall Figure 7, inset). The product solution was evacuated to dryness at ambient temperature; the Fischer-Porter bottle was disconnected from the hydrogenation apparatus and transferred back into the drybox. The dry reaction catalyst and residue were dissolved in 2.5 mL of Burdick & Jackson acetone followed by the addition of 0.5 mL of cyclohexene. The resulting 3.0 mL of solution was then divided equally into three 1.0 mL parts, which were placed into three new borosilicate culture tubes. Solution I was used in a Standard Conditions cyclohexene hydrogenation reaction as a standard for comparison; the reaction proceeded without an induction period and with an initial H_2-loss rate of 1.5 mmol of H_2/h. Solution II was treated with 70 μL of a acetone solution containing 3.81×10^{-3} mM PPh_3 (0.2 equiv relative to the amount of **1**). After the solution was stirred for 30 min inside the drybox in a septum-capped culture tube, the septum stopper was removed and the culture tube placed in a Fischer-Porter bottle; the bottle was then removed from the drybox and reattached to the hydrogenation

(63) Droege, M. W. Ph.D. Thesis, University of Oregon, Aug 1984; p 138.

apparatus. A cyclohexene hydrogenation reaction was then attempted using 40 psig H_2. No H_2 uptake was observed even after 3 h for this previously fully active catalyst, Figure 13.

(c) Hg Poisoning Tests. The Hg test was examined in considerable detail because it is one of the most useful and best accepted "homogeneous vs heterogeneous" catalysts tests.[17,21]

(i) Cyclohexene Hydrogenation Using Hg-Pretreated Precatalyst 1. In the drybox, 19.8 mg of **1** (3.3×10^{-3} mmol) was dissolved in 2.5 mL of acetone in a borosilicate culture tube (containing a 0.5 in. magnetic stir bar) to give a clear, bright-yellow solution. Elemental Hg (3 g, 0.015 mol; 4.5×10^2 equiv) was then added. After stirring vigorously for 3 h the solution of **1** and Hg, the previously yellow solution changed to orange, and some of the bright metallic Hg droplets became coated with a gray film. The excess Hg was removed by filtration, 0.5 mL of purified cyclohexene was added to the clear orange-yellow solution, and the borosilicate tube was placed inside a Fischer-Porter bottle, which was then sealed, removed from the drybox, and attached to the hydrogenation apparatus. The cyclohexene hydrogenation reaction was then initiated with 40 psig H_2 and vigorous shaking and stirring according to the Standard Conditions detailed earlier. After an induction period of 4 h (i.e., twice the normal time), a normal hydrogenation H_2 uptake rate of 1.2 mmol of H_2/h was gradually reached. This experiment demonstrates that the pretreatment of **1** with Hg does not prevent **1** from turning to active catalyst but that the presence of Hg does lead to a significantly, ca. 2-fold longer induction period (as expected for autocatalysis by low-level Ir nanocluster formation and, in the presence of Hg, its poisoning).

(ii) Cyclohexene Hydrogenation Using the Hg-Pretreated Active Catalyst Derived from 1. In the drybox, 20.1 mg (3.5×10^{-3} mmol) of **1** was dissolved in 2.5 mL of acetone in a borosilicate culture tube (containing a 0.5 in. magnetic stir bar) followed by the addition of 0.5 mL of purified cyclohexene to give a clear, bright-yellow solution. The borosilicate tube was placed inside a Fischer-Porter bottle, which was then sealed, removed from the drybox, and attached to the hydrogenation apparatus. The cyclohexene hydrogenation reaction was then initiated with 40 psig H_2 and vigorous shaking and stirring according to the Standard Conditions detailed earlier. After an induction period of 1.5 h, the reaction rate gradually reached a nearly constant, normal rate of 1.0 mmol of H_2/h. The reaction was stopped when 50% of cyclohexene was generated; at this point only ca. 35−40% (see Figure 7, inset) of **1** had evolved into the active catalyst. The Fischer-Porter bottle was disconnected from the hydrogenation apparatus and taken into the drybox. There, the reaction mixture containing the active catalyst was stirred with 3 g of Hg (0.015 mol; 4.3×10^2 equiv) for 1 h. The excess elemental Hg and some black-gray powder was removed by filtration, and the resultant clear-yellow solution was transferred into a 18 × 150 mm borosilicate culture tube. To the tube, 0.2 mL of additional, fresh cyclohexene was added to compensate for any loss of cyclohexene during the filtration step. The Fischer-Porter bottle was then sealed, removed from the drybox, and re-attached to the hydrogenation apparatus, and the hydrogenation reaction was restarted with 40 psig H_2 in the standard way. *The previously fully active catalyst was completely inactivated by Hg.* Interestingly, however, after an induction period of 1.6 h the remaining ca. 65−70% of precatalyst **1** evolved into an active hydrogenation catalyst (of 0.32 mmol of H_2/h, roughly $^1/_4$ of the normal hydrogenation rate). This experiment therefore also confirms the results in experiment (i) above (i.e., indicating that Hg treatment does not prevent the remaining precatalyst **1** from evolving into the active catalyst).

(iii) Attempted Cyclohexene Hydrogenation *in the Presence of Hg* Using a Sample of the Isolated, Active Catalyst Derived from 1. In the drybox, 20.2 mg (3.5×10^{-3} mmol) of **1** was dissolved in 2.5 mL of Burdick and Jackson acetone in a borosilicate culture tube (containing a 0.5 in. magnetic stir bar) followed by the addition of 0.5 mL of fresh cyclohexene to give a clear, bright-yellow solution. The culture tube was placed inside a Fischer-Porter bottle which was then sealed, removed from the drybox, and attached to the hydrogenation apparatus. The cyclohexene hydrogenation reaction was then initiated with 40 psig H_2 and vigorous shaking and stirring according to the Standard Conditions detailed earlier. The reaction was stopped when 50% of the expected total H_2 uptake (i.e., 50% of the cyclohexene hydrogenation) was completed. The Fischer-Porter bottle was disconnected from the hydrogenation line and returned to the drybox, where it was opened, and 3 g of Hg (0.015 mol; 4.3×10^2 equiv) was added to the reaction mixture (note: the excess Hg *was not* filtered off in this experiment). The Fischer-Porter bottle was then removed from the drybox, reattached via the quick-connects to the hydrogenation apparatus, and repressurized with 40 psig H_2 to see if the hydrogenation reaction would continue. No further hydrogen uptake was observed, even after 20 h, confirming that the hydrogenation reaction is completely suppressed in the presence of Hg.

(iv) Attempted Hydrogenation *in the Presence of Hg* Starting with the Precatalyst 1. In the drybox, 20.0 mg (3.5×10^{-3} mmol) of **1** was dissolved in 2.5 mL of acetone in a borosilicate culture tube (containing a 0.5 in. magnetic stir bar) followed by the addition of 0.5 mL of fresh cyclohexene to give a clear, bright-yellow solution. Elemental Hg (3 g; 0.015 mol, 4.3×10^2 equiv) was then added to the solution. The culture tube was placed inside a Fischer-Porter bottle, removed form the drybox, and attached to the hydrogenation apparatus. The cyclohexene hydrogenation reaction was then initiated with 40 psig H_2 and vigorous shaking and stirring according to the Standard Conditions detailed earlier. No cyclohexene hydrogenation was observed over 24 h, further confirming that the cyclohexene hydrogenation catalyst is completely poisoned in the presence of Hg.

(d) Attempted Recovery via CO as the Known Dicarbonyl, $[(OC)_2Ir{\cdot}P_2W_{15}Nb_3O_{62}]^{8-}$. To an amber acetone solution of $Ir_{\sim 190-450}$ nanocluster (2 mg/1 mL) in a Schlenk tube, equipped with a side arm and a Teflon stopper, was introduced 10 psig CO while swirling the solution. The solution was then reexamined after deposition onto a carbon-coated Cu grid by TEM. The same 20 Å Ir nanoclusters were observed, indicating that no insignificant formation of $[(OC)_2Ir{\cdot}P_2W_{15}Nb_3O_{62}]^{8-}$ had occurred. An examination of the IR confirmed that none of the dicarbonyl had formed (an authentic example of $[(OC)_2Ir{\cdot}P_2W_{15}Nb_3O_{62}]^{8-}$ was prepared from 1.0 mM **1** in acetone and 10−15 psig CO pressure, following our earlier method, ν_{CO} = 1996 and 2072 cm^{-1}).[8a,50]

Note, therefore, that it is crucial that one let **1** evolve fully into the active $Ir_{\sim 190-450}$ nanocluster catalyst before attempting this CO recovery experiment, since 2 equiv of CO readily replaces the 1,5-COD in **1** in leading to $[(OC)_2Ir{\cdot}P_2W_{15}Nb_3O_{62}]^{8-}$, and thus any unreacted **1** will be mistakenly interpreted as recovery of the "active catalyst". This is presumably one of the errors D. Lyon made[8b] leading to his erroneous report of recovery of the active cyclohexene hydrogenation catalyst derived from **1** as "100 ± 10%" of $[(OC)_2Ir{\cdot}P_2W_{15}Nb_3O_{62}]^{8-}$ (the quantitative parts of Lyon's experiment are almost surely in error as well[8b]).

(e) Attempted Recovery of the Active Catalyst via 1,5-COD Addition. In an experiment reported elsewhere (see pages 119−120[8a]), neither 1 equiv nor 210 equiv of added 1,5-COD (i.e., equivalents vs the starting concentration of **1**) yielded any re-formed **1** (as judged by the complete lack of any induction period characteristic of **1** in a cyclohexene hydrogenation experiment.)

(4) Additional Quantitative Studies of Cyclohexene Hydrogenation Starting with 1 as Precatalyst. (a) Using Different Sources of Acetone Solvent (Varying Primarily in Their H_2O Content). In these studies, 2.5 mL of Burdick & Jackson acetone (labeled as containing 0.2% water, i.e., 0.10 M or 85 equiv of H_2O vs **1**) was replaced by Baker acetone, which was labeled as containing 0.3% water (i.e., 0.15 M or 128 equiv of H_2O vs **1**), or was replaced by acetone "purified" by distillation from K_2CO_3 (this latter "purified" acetone in fact contained 0.42 M H_2O as determined using a literature water-sensitive dye method;[44] this corresponds to 357 equiv of H_2O vs **1**). The acetone distilled from K_2CO_3 also contains at least four impurities (presumably aldol-condensation products[46]) that can be detected by both GLC and MS (but which we have not been able to unequivocally identify structurally) and that make the reaction ca. 300% faster; see Table 2. GLC data: DB-1 capillary column, the temperature of the column was controlled by a temperature program with an initial temperature of 30 °C for 4.0 min, ramped at 10 °C/min to 120 °C and held there for 0 min, and then ramped at 30 °C/min to an final temperature of 240 °C and held there for 5.0 min, followed by cooling back to 30 °C. The injector temperature was 150 °C, and the detector temperature was 100 °C. Four impurities peaks were found (impurity A, at the retention time of 3.41 min; impurity B, 4.38 min; impurity C, 6.10 min; impurity D, 13.6 min; see Figure E, supplementary material; the GLC flow rate was ca. 0.3 mL/min and thus too low to measure

more exactly). MS data (i.e., major *m/e* peaks): impurity A, 43, 45, 62, 70, 73, and 88; impurity B, 39, 43, 50, 52, 53, 63, 77, and 78; impurity C, 38, 39, 40, and 41; impurity D, 39, 41, 43, 60 and 101; see Figure F, supplementary material. Use of the NIH-NBS mass spectral library (42 000 spectra) failed to identify any of the impurity peaks. (Further efforts here are planned.)

Using **1** as the catalyst precursor and the otherwise Standard Conditions cyclohexene hydrogenation experiment detailed earlier, quite variable induction periods and rates of hydrogenation were observed. The specific results (their induction periods and then H_2 uptake rates at the linear part of their H_2-pressure loss curves) as a function of the acetone source are summarized in Table 2 and graphically in Figure 14.

To confirm that water is primarily responsible for these differences, the two batches of Baker acetone (either used as received or distilled over K_2CO_3) were purified by distillation over $CaSO_4$, a recommended[45] drying agent for acetone. The results are presented in Table 2 under "Acetone Solvent (Source and Treatment)".

(b) With Added H_2O or HOAc. In the drybox, 20.0 ± 2.0 mg ((3.53 ± 0.35) × 10^{-3} mmol) of **1** was dissolved in 2.5 mL of acetone in a borosilicate culture tube to give the usual clear, bright yellow-solution. Next, a predetermined amount of degassed H_2O (80, 1180, 1660, or 5600 equiv vs **1**) or HOAc (4.3 or 6.1 equiv vs **1**) was syringed into the swirling solution followed by the addition of 0.5 mL (4.95 mmol) of fresh cyclohexene. The culture tube was placed in Fischer-Porter bottle, sealed, removed from the drybox, and attached via its quick-connects to the hydrogenation apparatus, and a cyclohexene hydrogenation reaction was initiated under the usual Standard Conditions and with 40 psig H_2. The reaction proved very sensitive to the amount of H_2O, and even more so to HOAc, with dramatically shortened induction periods and greatly increased H_2-uptake rates as summarized in Table 2. The results are also displayed graphically in Figures 15 and 16. A TEM was taken of the precipitate from the experiment with 61 equiv of HOAc to see if the size or the distribution of the Ir nanoclusters had dramatically changed. The results and associated size-distribution diagram (Figure D, supplementary material) demonstrate that neither the size (ca. 20 Å) nor the distribution of the Ir nanoclusters has changed significantly.

To rule out any effect due to the OAc^- counteranion, a control experiment involving a Standard Conditions hydrogenation beginning with **1** was done, except with the addition of 80 equiv of $Bu_4N^+OAc^-$. No change in the induction period nor the linear part of the H_2 curve was observed (Table 2), demonstrating that the effect of H^+OAc^- is due to its H^+.

The addition of 60 mg (66 equiv vs **1**) of Proton Sponge to a Standard Condition hydrogenation experiment did not change (i.e., did not decrease) the rate of hydrogenation, demonstrating that HOAc is *not* one of the acetone impurities (*vide supra*) which gives enhanced hydrogenation rates.

(c) Using Different Solvents. In these cyclohexene hydrogenation experiments, Burdick & Jackson acetone was replaced by CH_3CN, CH_2Cl_2, and $C_2H_4Cl_2$ solvents, each of which was prepurified by distillation from CaH_2 under N_2. In all cases a solution of 1.2 mM in **1** was prepared inside the drybox in a borosilicate culture tube (equipped with a 0.5 in. stir bar), using the Fischer-Porter bottle, 0.5 mL of fresh cyclohexene, and 40 psig H_2 and employing the other Standard Conditions and procedures described earlier.

The results, summarized in Table 2, proved quite different from those in acetone described so far and demonstrate that the generation and stability of the metastable $Ir_{\sim 190-450}$ polyosoanion nanocluster hydrogenation catalyst system is very sensitive to the solvent. In CH_3CN, black bulk Ir(0) metal particles (identified as such by electron diffraction) are observed within 1 h after the hydrogenation reaction was started. In $C_2H_4Cl_2$, a very long, ca. 7 h induction period is observed, followed by a ca. 50% slower H_2-loss rate (Table 2), results that were confirmed in two independent experiments. No cyclohexene hydrogenation occurred in CH_2Cl_2 even after 38 h, a results confirmed by D. Lyon.[8a] (Actually, Lyon reported *no* induction period in $C_2H_4Cl_2$,[8a] but a reanalysis of his data reveals a slower H_2 pressure decrease, followed by autocatalysis after ca. 17 h and a rate increase after 11 h. We believe that he misinterpreted a small pressure leak as the lack of an initial induction period, although it should also be noted that his reaction was run with 0.81 mM **1** and 1.1 M cyclohexene.)

Acknowledgment. Dr. D. K. Lyon is acknowledged for construction of the computer-interfaced hydrogenation apparatus described herein, for initial investigations of this system,[8] and for the control experiments cited along with his name in the Experimental Section. Dr. D. Edlund is similarly acknowledged for the early experiments with heterogeneous Ir(0) catalysts. Also acknowledged are Dr. Alessandro Trovarelli for his discussions of structure sensitivity and insensitivity, Dr. John Bradley (Exxon) for the colloid preparation references he supplied early in this project, and Drs. G. McVicker and R. Garten for providing the sample of 80% dispersed 1% Ir/η-Al_2O_3. Financial support was provided by the Department of Energy, Chemical Sciences Division, Office of Basic Energy, Grant DOE FG06-089ER13998.

Supplementary Material Available: Table A, a summary of previous approaches and studies of the "homogeneous vs heterogeneous catalysis problem"; Figure A, a plot of ln absorbance (A) vs r^2 from the ultracentrifugation molecular-weight determination for the $Ir_{\sim 190-450}$ nanoclusters; Figure B, a plot of ln absorbance (A) vs r^2 from the ultracentrifugation molecular-weight determination for the polyoxoanions included in the $Ir_{\sim 300}$ nanoclusters; Figure C, a visible spectrum of the $Ir_{\sim 300}$ nanoclusters in acetone; Figure D, a TEM of the Ir nanoclusters prepared during cyclohexene hydrogenation starting with 1.2 mM $(Bu_4N)_5Na_3[(1,5\text{-COD})Ir{\cdot}P_2W_{15}Nb_3O_{62}]$ and 1.65 M cyclohexene and with the addition of 61 equiv of HOAc in acetone under 40 psig H_2; Figure E, a GC trace of acetone which was stored over, and distilled from, K_2CO_3; Figure F, mass spectra of four impurity peaks found in acetone solvent stored over, and distilled from, K_2CO_3; and a brief discussion of the acetone impurities and their effect on the rate of cyclohexene hydrogenation (includes text, Table B, and Figure G) (12 pages). Ordering information is given on any current masthead page.